Theory of Rates of S_N2 Reactions and Relation to Those of Outer Sphere Bond Rupture Electron Transfers

R. A. Marcus

Noyes Laboratory of Chemical Physics, 127-72, California Institute of Technology, Pasadena, California 91125

Received: November 7, 1996; In Final Form: February 26, 1997[⊗]

A model is considered for S_N2 reactions, based on two interacting states. Relevant bond energies, standard electrode potentials, solvent contributions (nonequilibrium polarization), and steric effects are included. A unified approach is introduced in which there can be a flux density for crossing the transition state, which is either bimodal, one part leading to S_N2 and the other to ET products, or unimodal with a less marked energy-dependent separation of the rates of formation of these products. In a unified description an expression is given for the reorganization energy, which reduces in the appropriate limits to the pure S_N2 and ET/bond rupture cases. Expressions are obtained for the S_N2 rate constant and for its relation to that of the concerted electron transfer/bond rupture reaction. Applications of the theory are made to the cross-relation between rate constants of cross and identity reactions, experimental entropies and energies of activation, the relative rates of S_N2 and ET reactions, and the possible expediting of an outer sphere ET reaction by an incipient S_N2-type interaction. Results on the photoelectron emission threshold energies of ions in solution provide some information on a solvation term, and another quantity can be estimated using data from gas phase S_N2 reactions or from quantum chemistry calculations. Also introduced for comparison is an adiabatic model that is an extension of a bond energy−bond order formulation for gas phase reactions.

I. Introduction

A subject of continuing interest is the detailed mechanism of S_N2 and related electron transfer (ET) reactions and the relation between them:[1−5] If $A^{\bullet-}$ and A^- denote a radical anion and an anion such as a carbanion, or other electron donor, such as an electrode, one type of electron transfer reaction, frequently termed "outer sphere," is

$$A^- + RX \rightarrow A^\bullet + R^\bullet + X^- \qquad \text{ET} \qquad (1a)$$

or

$$A^{\bullet-} + RX \rightarrow A + R^\bullet + X^- \qquad \text{ET} \qquad (1b)$$

where R is an organic group and X is usually but not necessarily a halide. A treatment of the concerted ET/bond rupture reactions 1a and 1b was given by Savéant,[6] using Morse and Morse-like repulsive curves for RX and $R^\bullet X^-$, respectively.

An S_N2 mechanism of the electron transfer type, on the other hand, is described by

$$A^- + RX \rightarrow AR + X^- \qquad S_N2 \qquad (2a)$$

or

$$A^{\bullet-} + RX \rightarrow AR^\bullet + X^- \qquad S_N2 \qquad (2b)$$

We consider S_N2 reactions in solution, using a two-interacting-states model. This treatment differs from one introduced for comparison in Appendix A. The latter is an extension of Johnston's[7] BEBO (bond energy−bond order) model for S_N2 reactions of neutrals to those of the ET type. The present two-interacting-states model is motivated, in part, by trying to explain why reactions 1 and 2 sometimes have somewhat comparable rates while for other systems they can differ by 20 orders of magnitude. Other experimental observations, discussed later, also stimulated the present treatment.

Reaction 1 may occur in a concerted or sequential manner and in either case be followed by reactions of the products. These products may, in turn, react before or after escaping from the solvent cage, depending upon the system. Many studies have been made of the effect of varying the various reactants, the solvent, and, when A is an electrode, the electrode−solution potential difference. When RX is sterically hindered toward an attack by A^- on the C in the ⩾C−X bond in RX in reaction 2, that reaction tends to become reaction 1. That trend is also expected when the A−R bond is sufficiently weak.

Stereochemistry has played a significant role in studies of the reaction mechanism, inasmuch as 100% inversion implies an S_N2 reaction mechanism only, while partial inversion can imply the operation of both mechanisms, as in stereochemical studies of the reaction of anthracene radical anions with optically active 2-octylhalides.[8] Other techniques such as measuring certain ratios of products have also established the ratio of reactions 1 and 2 rate constants, for example for anthracene radical anions reacting with methyl halides.[9]

Another feature of S_N2 reactions is the "cross-relation", which relates rate constants of "cross-reactions" to identity reactions (a relation that played a prominent role[10,11a,c] in the interaction of theory and experiment for electron transfer reactions). This relation has also been applied to S_N2 and other reactions.[1,5]

There is also a large body of experimental studies comparing rate constants for S_N2 and ET reactions, their activation energies and activation entropies, and also the competition of the two types of reaction within the same system (e.g., refs 1−5 and 9). Extensive experimental studies have also been made of gas phase S_N2 reactions.[4d,12] A comparison of their barriers with those of S_N2 reactions in solution provides information on solvent effects and is discussed in a subsequent section.

The paper is organized as follows: In section II, some general comments are made on factors that the theory should incorporate. A unified pictorial description of S_N2 and concerted ET/

[⊗] Abstract published in *Advance ACS Abstracts,* April 15, 1997.

S1089-5639(96)03722-X CCC: $14.00

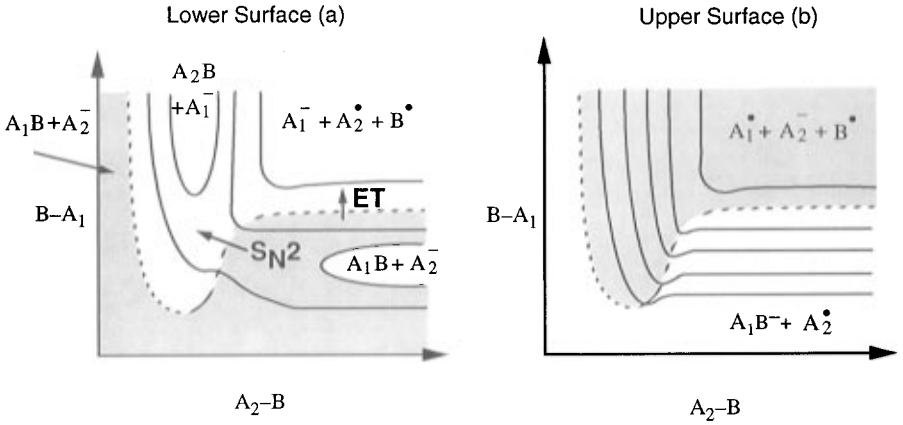

Figure 1. Schematic contour plot of the upper and lower potential energy surface for a reaction in which only two electronic states need be considered in the fully separated species. In one of these (the shaded region) the extra charge is localized on A_1^- and in the other on A_2^-. The dotted line indicates the TS. As indicated by the arrows, crossing it in one region corresponds to an S_N2 mechanism and crossing it in another to a concerted ET/bond rupture. There is a substantial "splitting" of two surfaces (a and b) in the vicinity of the dotted line region,[1] when both A_1B and A_2B distances are small, and there can be an admixture of other electronic configurations, such as $A_1^-B^+A_2^-$ and $A_1^{\bullet}B^-A_2^{\bullet}$, in the TS region. There is a saddle-point (not shown) on the lower surface, near the center of the S_N2 arrow.

bond rupture reactions is then given. The S_N2 limit is treated next, including both the reorganization energy and the partition function factor. (These two aspects, together with transition state theory, yield an expression for the rate constant.) A functional form is then suggested for the "resonance energy" of the two states, one that provides a bridge between the two types of reactions. An expression for the S_N2 rate constant is obtained, and the case of the outer sphere concerted ET/bond rupture reaction[6] is then recalled for comparison and shown to be a limiting case of the present unified treatment. It is next shown from the expression for the reorganization energy how an incipient S_N2-type interaction may expedite the concerted ET/bond rupture reaction.

In section III applications are made to several phenomena or deductions, to experimental data on the cross-relation for S_N2 reactions, the relation of the S_N2 and ET rate constants, entropies of activation of S_N2 and ET reactions, the effect of the standard free energy of reaction on the rate constant, and the use of gas phase S_N2 data to obtain information for application to solution phase S_N2 reactions. We conclude with some remarks on computer simulations, on applications of quantum chemical calculations, and on nonequilibrium polarization. An adiabatic formulation, an extension of the BEBO treatment for S_N2 reactions of neutrals, is given in the Appendix.

II. Theory

Introduction. We recall that in a reaction the reactants diffuse toward each other to form (for convenience of calculation at least) an "encounter complex" R from which they react. Reaction then leads to an "encounter complex" P of the products and thence by diffusion to the separated products. In the present paper we focus on the process leading from R to P and then calculate the bimolecular reaction rate constant by assuming, in effect, a pre-equilibrium for R. If the diffusion from the separated reactants to form R, or from P to yield the separated products, becomes sufficiently slow, the calculation below also provides a unimolecular rate constant for the R → P process, upon dividing the bimolecular rate constant by the equilibrium constant for forming the encounter complex R. This unimolecular rate constant then serves as a boundary condition for the solution of the diffusion equation.

In treatments of S_N2 reaction rates it is desirable to include factors such as the following:

(i) The energy barrier arising from the bond rupture is decreased by formation of a new bond. Indeed, in gas phase metathesis reactions of neutrals this effect can reduce the energy barrier by a factor of about 10 or so in some systems.[7]

(ii) The S_N2 reactions have a larger steric effect than the outer sphere electron transfers. The magnitude of this effect is expected to depend on whether the transition state (TS) is reactants-like, products-like, or in between.

(iii) Solvent effects typically increase the S_N2 reaction barrier relative to its value in the gas phase. Some partial desolvation, with an accompanying increase in energy barrier, is expected to accompany the formation of the TS, since the charge in the TS is delocalized over a relatively large system, rather than being localized on a smaller system, the A^- in eq 2. This effect is the usual static solvent effect. When the charge distribution in the TS is dominated by two very different contributions, a nonequilibrium polarization of the solvent may occur: the polar solvent molecules are slow moving and cannot be appropriately oriented to each of the two different contributions to the charge distribution. This effect is particularly marked for weak-overlap electron transfer reactions not involving bond rupture and in fact is a cornerstone of that theory.[10,11] It is the counterpart for these systems of the conventional static partial desolvation involved in formation of the TS.

There has been extensive discussion in the literature, using both stereochemistry and activation energies and entropies, of the relation between the S_N2 reactions 2 and the ET reactions 1. We shall consider how that discussion, which we describe below, can be phrased pictorially in terms of the crossings of different parts of a single transition state "hypersurface" (Figure 1). (The hypersurface is a surface of $N - 1$ dimensions that separates the reactants' from the products' spatial regions (or phase space) of the N-dimensional space.)

The model for an S_N2 reaction considered below involves two interacting states, with a resonance energy lowering of the energy barrier.[13] In the model the three items listed above are treated using a nonequilibrium solvent polarization for item iii. The two-state description of the transition state (TS) of this reaction can be regarded as corresponding to a mapping of the results of a multistate (not merely two-state) electronic configuration calculation in the vicinity of the TS onto a two-state description. A mapping onto two states has been suggested in the literature.[14]

When this resonance energy β is unusually large, the use of two diabatic states as a starting point may not be as good as employing an adiabatic model, an example being the Finklestein reaction discussed later. However, it can still be useful for our purpose. In many other cases described later, this resonance

energy lowering is much less. A virtue of a two-interacting-state model is that it provides a simple basis for developing a unified description of the two types of reaction and, we believe, insight as to why the rates sometimes differ by less than an order of magnitude. The model is less valid for some S_N2 reactions, those whose resonance energy lowering is so large that other zeroth-order states are almost certainly mixed in.

Potential Energy Surface. It is useful to consider first what the potential energy surface might look like for an S_N2 reaction,

$$A_2^- + BA_1 \rightarrow A_2B + A_1^- \quad (3a)$$

or

$$A_2^{\bullet -} + BA_1 \rightarrow A_2B^{\bullet} + A_1^- \quad (3b)$$

and for an ET reaction

$$A_2^- + BA_1 \rightarrow A_2^{\bullet} + B^{\bullet} + A_1^- \quad (4a)$$

or

$$A_2^{\bullet -} + BA_1 \rightarrow A_2 + B^{\bullet} + A_1^- \quad (4b)$$

In the interests of brevity we shall use eqs 3a and 4a as examples, as in Figure 1, but all such descriptions are intended to apply to eqs 3b and 4b as well, simply by replacing A_i^- by $A_i^{\bullet -}$.

A potential energy surface is sketched schematically in Figure 1 as a function of the A_1B and A_2B distances. In this Figure, two electronic states are considered for the fully separated systems in the solution, $A_2^- + A_1^{\bullet} + B^{\bullet}$ and $A_1^- + A_2^{\bullet} + B^{\bullet}$. For concreteness, the energy of the latter is taken to be lower than that of the former. The lower of the two adiabatic potential energy surfaces is depicted in part a of Figure 1 and the upper adiabatic surface in part b. In each case the shaded region is intended to indicate an electronic configuration where the charge is centered mainly on the A_1^-, while in the unshaded region it is mainly on the A_2^-.

The dotted line borderline region is composed of contributions from both electronic configurations (and from others) and serves approximately as the transition state (TS). In the dotted line region there is a large splitting (avoided crossing) of the two potential energy surfaces when both A_1B and A_2B distances are small. The splitting becomes small, presumably exponentially so, when either of those distances becomes large. There are, of course, many more coordinates, including the coordinates of the solvent molecules. They are included in the formulation, and the dotted line in Figure 1 is intended to represent an $(N-1)$-dimensional TS hypersurface in the N-dimensional space. A connection with computer simulations is discussed in a later section.

The system can cross from the reactants' to the products' region at any place on the dotted line TS. In crossing one part the reaction corresponds to an S_N2 reaction, reaction 3, while in crossing another part it corresponds to an outer sphere concerted ET/bond rupture reaction, reaction 4. The former involves passage across the lower energy regions of the dotted line in Figure 1a, and so has a lower activation energy and is indicated by an S_N2 arrow, while the ET occurs across an upper region of the dotted line in Figure 1a and is indicated by the ET arrow. In some intermediate region of the dotted line reactive trajectories could end in either product region.

Two views have been expressed in the literature regarding the ET and S_N2 reactions: They occur on the same potential energy surface and (i) are competitive,[2b,8,13,15,16] or (ii) the behavior is one that varies continuously between these two limits.[3,4c] These two views can be described pictorially with the aid of Figure 1, in terms of the flux density across the dotted line: If separate ET and S_N2 paths contribute, then this flux density is bimodal, with one peak in the S_N2 path region in Figure 1a and a second peak in the ET path region there. If, instead, there is only one peak in the flux density across the TS dotted line, i.e., if a unimodal behavior occurs, the flux will be concentrated either along the S_N2 path or, for other systems, along the ET path or, for still others, along some in between path across the dotted line. In that last unimodal case some crossing trajectories could end up in the S_N2 region of the products, either directly or by stabilization of a transient S_N2-like "intermediate," and some in the ET region, again either directly or by dissociation of that intermediate.[16]

It is convenient initially to treat the two paths labeled by ET and by S_N2 in Figure 1a separately and then to show how these paths are limits of a unified treatment. In the latter, crossings of other parts of the dotted line region are included, namely, in the region between the two arrows. Indeed, this latter crossing could prove to be an ingredient in explaining some observations mentioned later.

Not shown in Figure 1a is another TS, namely, for a different reaction, the ET reaction between nearby separated particles A_1^- and $A_2^{\bullet}$ to form $A_1^{\bullet}$ and A_2^-. Here, x_1 and x_2 are both large, but only because $B^{\bullet}$ is far removed from the other two particles. The TS for this reaction is along the line $x_1 = x_2$ in Figure 1a, with, at the same time, $A_1^{\bullet}$ and A_2^- being close together and with there being a suitable fluctuation of the solvent coordinates to permit this ET to occur. To describe this reaction requires an additional coordinate, in an $A_1^-A_2^{\bullet}$ encounter complex, a fluctuation coordinate analogous to but different from the Y introduced in eqs 5 and 6 below. Each of these fluctuation coordinates is related to a molecular coordinate ΔU_s, described in a later section of this article, each ΔU_s being chosen for each reaction studied.

The model for the S_N2 reaction is formulated next.

Two-Interacting-States Model. In an extension of electron transfer theory to ET reactions accompanied by bond rupture Savéant[6] employed a Morse potential energy function $D_1[1 - \exp(-a_1x_1)]^2 - D_1$ for the rupturing bond RX in reaction 1a or 1b. Here, x_1 denotes the bond distance displacement from its equilibrium value in RX. He also assumed for the repulsion term between $R^{\bullet}$ and X^- the quantity $D_1 \exp(-2a_1x_1)$. (The repulsion arises from the Pauli exclusion principle [cf. ref 17, valence bond theory, and ref 7a].) There was an experimental basis for the exponential modeling of the repulsion, namely, in the experiments and interpretation of Wentworth and co-workers of experiments on electron attachment to gas phase alkyl halides.[18] The D_1 includes the effect of the change of bond angles from tetrahedral in RX to planar trigonal in $R^{\bullet}$. (Cf. also ref 12 of ref 6.) We shall use similar ideas for S_N2 reactions.

To treat the S_N2 reaction 3, we introduce in Figure 2 a free energy bookkeeping diagram. (Free energy curves were used in ET reactions, e.g., refs 10, 11, 19.) One contribution to the free energy change for forming the TS from the encounter complex R of the reactants is denoted there by ΔG_r. Treated separately are contributions due to changes in rotational−vibrational partition functions Q. We first remark on the various free energy changes depicted in Figure 2: The free energy change from the separated reactants to the reactants' encounter complex R is denoted by $w_r - k_BT \ln q_{rot}^{(2)}q_{vib}^{(1)}/q_{trans}^{(3)}$, where the superscripts indicate the number of coordinates involved, and w_r is the interaction free energy of A_1B and A_2^- in the encounter complex R ("work term"). (The equilibrium constant K_r for

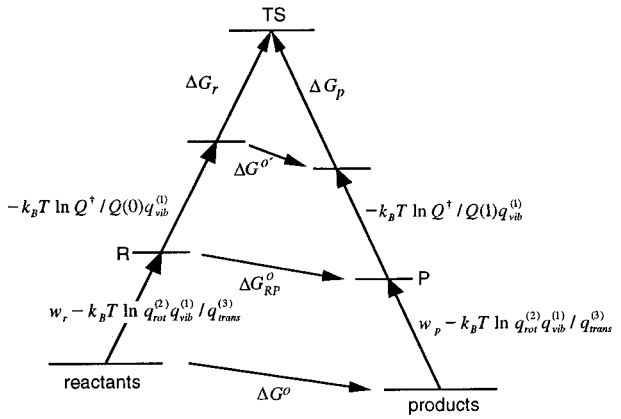

Figure 2. Diagram of free energy changes and definitions for an S_N2 reaction. The various symbols are defined in the text.

forming R would be obtained by setting $-k_BT \ln K_r$ equal to the above free energy change.) The $q_{rot}^{(2)}$, $q_{vib}^{(1)}$, $q_{trans}^{(3)}$ are defined in ref 20.

The displacement of the A_iB bond length from its equilibrium value in A_iB is denoted by x_i. The changes in (x_1, x_2) occur from R to the products' encounter complex P, rather than before R or after P. The quantities $Q(0)$, $Q(1)$, and $Q^\dagger$ are defined by setting $Q(0)q_{trans}^{(3)}$, $Q(1)q_{trans}^{(3)}$ and $Q^\dagger q_{rot}^{(2)}$ equal to the partition functions for the reactants, the products, and the TS, respectively. The first $q_{trans}^{(3)}$ is that for the reactants, in the center of mass system of coordinates, the second is that for the products, and the $q_{rot}^{(2)}$ is that for the reactants. This choice of notation for the Q's is introduced in order to yield simpler expressions later on. $Q(0)$, $Q(1)$, and $Q^\dagger$ contain the same number of coordinates.

For ΔG_r, the free energy of formation of the state (X_1, X_2, Y) from R, excluding the Q and $q_{vib}^{(1)}$ terms (cf. Figure 2), we write

$$\Delta G_r = D_1(X_1 - 1)^2 + D_2 X_2^{\,2} + \lambda_0 Y^2 \qquad (5a)$$

where

$$X_i = \exp(-a_i x_i), \quad \lambda_0 = \lambda_0(X_1, X_2)\ (i = 1, 2) \qquad (5b)$$

and x_i refers to the $B-A_i$ bond displacement coordinate. In eq 5 there is a solvent fluctuation term $\lambda_0 Y^2$, in which a generalized fluctuation coordinate Y is introduced whose equilibrium value is 0 for the reactants' state and 1 for the products. The λ_0 in eq 5 will later prove to have its usual significance as a reorganization energy. The λ_0 in $\lambda_0 Y^2$ may be a function of (X_1, X_2), since the geometry of the solute depends on (X_1, X_2) and is assumed to be slowly varying.

The $D_1(X_1 - 1)^2$ term in eq 5 describes the interaction between A_1 and B in A_1B, and the $D_2X_2^2$ term denotes the repulsion between A_1B and A_2^-. As noted earlier the D_1 and D_2 include the effect of the changes in bond angles. We should keep open the option, should future quantum chemistry calculations support it, of adding a positive term linear in X_2 to eq 5a and, in eq 6 below, linear in X_1.

There will also be some solvent caging effect, but from an energetics point of view its effect on eq 5 is expected to be relatively minor. Its effect should be mainly on the diffusion aspects of the problem, when diffusion to R from ∞ or from P to ∞ becomes slow. The molecular counterpart of Y is an energy difference coordinate ΔU_s discussed in a later section.

We write a similar expression for ΔG_p for forming the state (X_1, X_2, Y) from the products' encounter complex P, again excluding the Q and $q_{vib}^{(1)}$ terms in the definition,

$$\Delta G_p = D_1 X_1^{\,2} + D^2(1 - X_2)^2 + \lambda_0(1 - Y)^2 \qquad (6)$$

In a two-interacting-states model the electron transfer occurs, in the first approximation, at the "intersection" of the two free energy curves.[10,11,19] Thereby, the free energies G_r and G_p are equal, and it follows (Figure 2) that

$$\Delta G_r - \Delta G_p = \Delta G^\circ_{RP} + k_B T \ln Q(1)/Q(0) \equiv \Delta G^{\circ\prime} \qquad (7)$$

where ΔG°_{RP} is related to the standard free energy of reaction ΔG° as in eq 9 below and as depicted in Figure 2.

The standard free energy of reaction ΔG° of reaction 3 is given in terms of standard potentials E°, the D's, and partition functions as

$$\Delta G^\circ = E^\circ_{A_2^\bullet/A_2^-} - E^\circ_{A_1^\bullet/A_1^-} - D_{A_2B} + D_{A_1B} - k_B T \ln Q_{A_2B} Q_{A_1^\bullet} / Q_{A_1B} Q_{A_2^\bullet} \qquad (8)$$

where $E^\circ_{A_2^\bullet/A_2^-}$ is the standard potential of the half-cell reaction $A_i^\bullet + e \rightarrow A_i^-$, and the Q's denote the partition functions of the cited species. Since the reactions are occurring in solution, the minor distinction between Gibbs and Helmhotz free energies can be ignored throughout.

As one sees from Figure 2, the standard free energy of reaction from R to P, ΔG°_{RP}, is related to ΔG° by

$$\Delta G^\circ_{RP} = \Delta G^\circ + w_p - w_r - k_B T \ln[q_{rot}^{(2)} q_{vib}^{(1)} / q_{trans}^{(3)}]_p / [q_{rot}^{(2)} q_{vib}^{(1)} / q_{trans}^{(3)}]_r \qquad (9a)$$

where the subscript p or r denotes the encounter complex to which the $q_{rot}^{(2)} q_{vib}^{(1)} / q_{trans}^{(3)}$ terms refer. Hence,

$$\Delta G^\circ_{RP} = E^\circ_{A_2^\bullet/A_2^-} - E^\circ_{A_1^\bullet/A_1^-} - D_{A_2B} + D_{A_1B} + w_p - w_r \qquad (9b)$$

where partly for simplicity of notation we have canceled the partition function ratios that appear in eqs 8 and 9, probably with minor approximation, since the $A_i^\bullet$ and A_iB in eq 8 are neutrals. One can always reintroduce them in order to calculate ΔG°_{RP}.

The TS should be located by minimizing $\Delta G_r - k_B T \ln Q^\dagger$, subject to the constraint imposed by eq 7. A variational parameter would be introduced into $Q^\dagger$ for this purpose. We return to this point later. For the moment we treat the variation of $Q^\dagger$ along the reaction path as "slow" and include that variation later in an approximate way. The G_r and G_p surfaces in the (X_1, X_2, Y) space intersect, and we find the lowest point on the intersection by minimization of ΔG_r in eq 5a, subject to the constraint imposed by eq 7, and treating $\lambda_0(X_1, X_2)$ as a slowly varying function of (X_1, X_2). We obtain, in terms of a Lagrangian multiplier m,

$$X_1 = m + 1, \quad X_2 = -m, \quad Y = -m, \quad 2m + 1 = -\Delta G^{\circ\prime}/\lambda \qquad (10)$$

We thus find, with $\Delta G^{\circ\prime}$ given by eqs 7 and 9b,

$$\Delta G_r^* = \frac{\lambda}{4}\left(1 + \frac{\Delta G^{\circ\prime}}{\lambda}\right)^2 - \beta_{ij} \qquad (11)$$

where

$$\lambda = \lambda_0 + D_{A_1B} + D_{A_2B} \equiv \lambda_0 + \lambda_i \qquad (12)$$

and we have now included the resonance energy β_{ij} of interaction of the states $(i, j = 1, 2)$. The second half of eq 12 also serves to define λ_i. The λ_0 in eq 12 is the change in solvation energy

accompanying a vertical transition $A_i^-BA_i \rightarrow A_iBA_i^-$, using the $A_iBA_i^-$ geometry in the TS. The distortion of the free energy by the β_{ij} interaction may cause the TS not to lie exactly where the free energies of the two undistorted states are equal.

We will assume that the resonance energy β_{ii} of an identity reaction ($A_i = A_j$) is proportional to some property denoted by D_i', which is to be chosen later and which depends on the A_iB interaction. Since β_{ii} should also decrease exponentially with x_i, we shall also take it as proportional to X_i^{2l} where l is some power or fractional power. In the case of a nonidentity reaction, β_{ij} depends on both the A_iB and BA_j interactions, and we will assume that it is proportional to $(D_i'D_j')^{1/2}$ and that it decreases exponentially with x_1 and x_2, namely, it is proportional to $(X_iX_j)^l$.

In summary, we assume

$$\beta_{ii} = \gamma_i D_i' \tag{13a}$$

$$\beta_{ij} = (\gamma_i\gamma_j D_i' D_j')^{1/2}(4X_iX_j)^l \tag{13b}$$

where a typical l is to be determined from some quantum chemistry estimate. (Alternatively, an arithmetic mean, rather than a geometric one, might be more appropriate.) Equation 13b reduces to 13a in the case of $i = j$, since $D_i' = D_j'$, $\gamma_i = \gamma_j$, and $X_i = X_j = 1/2$ then. The l in eq 13b may be on the order of unity: In a chemical bond, two electrons are involved, and at larger distances this interaction, which can be regarded roughly as a resonance energy of the separated atoms, involves two electrons and varies (Morse potential at larger x_i) as X_i and at negative x_i as X_i^2. Diatomic Coulombic and exchange integrals have indeed been expressed in terms of the X_i's.[7d] In $A_iBA_j^-$ four electron integrals replace the two electron ones, and so β_{ij} may be proportional to $(X_iX_j)^l$, where l is perhaps *ca.* 1 to 2 instead of 1/2 to 1. Quantum chemistry calculations of the potential energy surfaces will permit the testing of the appropriate functional form for β_{ij}.

From eq 10 one finds that X_1X_2 equals $-m(m+1)$, i.e., $(1/4)(1 - \Delta G^{\circ\prime}_{S_N2}/\lambda_{S_N2})^2$ at the TS of the S_N2 reaction. We have, thereby, from eq 13b,

$$\beta_{ij} = (\gamma_i D_i'\gamma_j D_j')^{1/2}[1 - (\Delta G^{\circ\prime}_{S_N2}/\lambda_{S_N2})^2]^l \quad \text{(at the } S_N2 \text{ TS)} \tag{13c}$$

In an application to the cross-relation, we shall approximate the geometric mean in eq 13c by the arithmetic mean. With this subsequent step in mind eq 13c is rewritten as

$$\beta_{ij} = {}^1/_2\{[\gamma_i D_i' + \gamma_j D_j'] - [(\gamma_i D_i')^{1/2} - (\gamma_j D_j')^{1/2}]^2\}[1 - (\Delta G^{\circ\prime}_{S_N2}/\lambda_{S_N2})^2]^l \quad \text{(at the } S_N2 \text{ TS)} \tag{13d}$$

The term involving the difference of the square roots will be neglected when $(\gamma_i D_i')^{1/2}$ and $(\gamma_j D_j')^{1/2}$ are not too different.

The rate constant is next evaluated using transition state theory:[20a]

$$k = \frac{k_B T}{h} e^{-\Delta G^\dagger/k_B T} \tag{14}$$

We note, in passing, that for reactions in solution there is some coupling between the solvent coordinates and the vibrational−rotational coordinates of the solute that participate in the Q's, even though we later approximate the Q's by their gas phase values. The solvent and solute coordinates are also coupled to the motion along the reaction coordinate, so permitting the system to surmount the reaction barrier.

The $\Delta G^\dagger$ can be written as the sum of ΔG_r^* given by eq 11, the work term w_r, and the partition function term, $-k_BT \ln Q^\dagger q_{rot}^{(2)}/Q(0)q_{trans}^{(3)}$. The $q_{rot}^{(2)}/q_{trans}^{(3)}$ and the k_BT/h contribute to $(k_BT/h)\exp(-\Delta G^\dagger/k_BT)$ a factor denoted by Z,[20b] a "collision frequency". We thus obtain

$$k_{S_N2} = Z[Q^\dagger/Q(0)]\exp(-\Delta G^*_{S_N2}/k_BT) \tag{15}$$

where

$$\Delta G^*_{S_N2} = w_r + \Delta G_r^* \cong w_r + \frac{\lambda_0 + D_1 + D_2}{4} - \beta_{ij} + \frac{\Delta G^{\circ\prime}}{2} + \frac{\Delta G^{\circ\prime 2}}{\lambda} \tag{16}$$

$\Delta G^{\circ\prime}$ is given by eq 9b and the second half of eq 7, β_{ij} by eq 13c, and the sum in the second term on the right is $\lambda/4$ (cf. eq 12). Strictly speaking, the pre-exponential factor Z in eq 15 will be somewhat larger than in ref 20b, when a distribution function is introduced for the pair of the reacting solutes in the liquid.[21]

We consider next the factor $Q^\dagger/Q(0)$. A large moment of inertia in R, written[20b] as $\mu\sigma^2$, enters into $q_{rot}^{(2)}$, and from it into Z. The corresponding moment of inertia in the S_N2 TS is somewhat smaller than it is in R. We can include this effect by defining a Z_{S_N2}/Z, which is the ratio of these moments of inertia, and employing this Z_{S_N2} in eq 19 below. We consider next the remaining factors appearing in $Q^\dagger/Q(0)$. They are associated with the conversion of individual rotations of the reactants into bending vibrations of the TS. Typically, $\Delta G^{\circ\prime}/\lambda$ is relatively small: a $\Delta G^\dagger$ *vs* ΔG° plot for the S_N2 reaction is frequently linear with a slope near 0.5 ± 0.1, and the configurations of the TS (e.g., Y, X_1, X_2) are roughly midway between those of the reactants and the products. In this case it is expected that $Q^\dagger$ have the value Q_T, estimated later, for a tight TS. One question is whether, when $\Delta G^{\circ\prime}/\lambda$ approaches -1 and the TS becomes, energetically, reactants-like, the $Q^\dagger$ (apart from the Z_{S_N2}/Z) approaches $Q(0)$. Similarly, when $\Delta G^{\circ\prime}/\lambda$ approaches $+1$ and the TS becomes, energetically, products-like, does $Q^\dagger$ approach $Q(1)$? If the answer to both questions is yes, then one possible interpolation for $Q^\dagger$ between these three points is

$$Q^\dagger/Q_T \cong (Q(0)/Q_T)^{|n|}(Z_{S_N2}/Z) \qquad -1 \le n \le 0 \tag{17a}$$

$$\cong (Q(1)/Q_T)^{|n|}(Z_{S_N2}/Z) \qquad 0 \le n \le 1 \tag{17b}$$

where

$$n = \Delta G^{\circ\prime}/\lambda \tag{18}$$

For describing the Q for a tight TS, Q_T, we first denote by q_{rot} an individual reactant's rotational partition function that becomes a vibrational partition function q_{vib} in the tight TS. Inasmuch as the polyatomic typically nonlinear reactants have three rotations each and the transition state has three, it follows that three of the reactants' rotations have become vibrations in the transition state, in the case of a tight TS. We have, thereby,

$$Q_T/Q(0) = (q_{vib}/q_{rot})^3 \tag{19}$$

and when $\Delta G^{\circ\prime}_{RP}/\lambda$ is relatively small, eqs 15−19 yield

$$k_{S_N2} = Z_{S_N2}(q_{vib}/q_{rot})^3\exp(-\Delta G^*_{S_N2}/k_BT) \tag{20}$$

with $\Delta G^*_{S_N2}$ given by eq 16. Of course, not all of the q_{vib}'s need be equal, nor all of the q_{rot}'s, but the notation in eqs 19 and 20 is convenient and suggestive, and in the application below we do not assume any equality of the q_{rot}'s or of the

q_{vib}'s. When n in eqs 17 and 18 approaches ± 1, and so $Q^\dagger$ approaches $Q(0)$ or $Q(1)$, apart from a Z factor, the TS becomes loose, and the pre-exponential factor in eq 15 could then become substantially larger, for example by a factor of 100 (cf. an estimate for Q_T later). Another effect of steric hindrance, besides leading to eq 19, is an energy of distortion effect reflected in part in the value of D_2, the energy of the newly formed bond in reaction 3. Steric hindrance reduces the magnitude of D_2.

The calculation of λ_0 for the $A_iBA_j^-$ system in the TS involves describing the geometry of the solute and then making a nonequilibrium polarization calculation. One useful experimental quantity is the λ_0 for a single ion $\lambda_0(A_i^-)$, obtained from the threshold energy E_t of the photoelectron emission by the ion in solution.[22] If $G^{e,sol}_{A_i^-} - G^{e,sol}_{A_i^\bullet}$ is the difference of equilibrium solvation free energies of $A_i^\bullet$ and A_i^-, then a thermodynamic cycle shows that $\lambda_0(A_i^-)$ is obtained from[22a]

$$\lambda_0(A_i^-) = E_t + G^{e,sol}_{A_i^-} - G^{e,sol}_{A_i^\bullet} - E_{A_i} \qquad (21)$$

where E_{A_i} is the electron affinity of $A_i^\bullet$. If A_i^- is, instead, an ion of arbitrary charge, the same equation applies, with $A_i^\bullet$ now denoting an A_i with one less negative charge than the ion in question.

Using a linear response approximation, we also note that the λ_0 for any geometry and any initial charge distribution can be calculated from a difference of equilibrium solvation free energies,[22b]

$$\lambda_0 = G^{e,sol}_{1-0} - G^{e,op}_{1-0} \qquad (22)$$

where the 1 denotes the final charge distribution after a vertical transition (in the present case after loss of the electron) and 0 denotes the initial charge distribution, so that $1-0$ denotes the difference of the two charge distributions. The e,op superscript denotes the equilibrium solvation but where only the electronic polarizability of the solvent enters rather than the total (electronic plus the nuclear) contributions.

In concluding this section we briefly comment on an implication of the preceding equations for the symmetric stretching force constant k_{sym} in the $A_iBA_i^-$ TS for the identity reaction, compared with the related stretching force constant k_s of A_iB. The symmetric stretching coordinate in the TS is $x = (1/\sqrt{2})(x_1 + x_2)$, i.e., $\sqrt{2}x_1$ along the line $x_1 = x_2$. Using eq 5, and introducing a β_{ii} given by eq 13b, we set $\partial(G_r - \beta_{ii})/\partial x = 0$ to locate the minimum along that $x_1 = x_2$ line. The desired force constant is $\partial^2(G_r - \beta_{ii})/\partial x^2$, k_{sym}, calculated at that minimum. Here, $G_r = D_1(X_1 - 1)^2 + D_1X_1^2 - D_1$, since $X_1 = X_2$ along the line. One finds

$$k_{sym} = a_i^2 D_i \quad (l = 1) \qquad (23)$$

$$k_s = 2a_i^2 D_i \qquad (24)$$

We have written eq 23 for the choice of $l = 1$ in eq 13b, for simplicity, but another l can readily be introduced instead.

Outer Sphere Concerted ET/Bond Rupture Reaction. To compare the above results with those obtained[6] for the ET/bond rupture reaction 4, we first recall briefly a derivation[6] of the rate expression. We consider first the standard free energy of reaction. The ΔG° of reaction 4 can be expressed in terms of the standard electrode potentials, a bond energy, and partition functions Q:

$$\Delta G^\circ = E^\circ_{A_2^\bullet/A_2^-} - E^\circ_{A_1^\bullet/A_1^-} + D_{A_1B} - k_BT \ln Q_{A_1^\bullet}Q_{B^\bullet}/Q_{A_1B} \qquad (25)$$

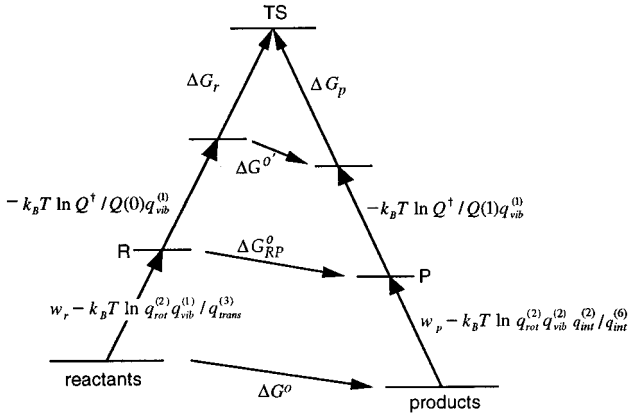

Figure 3. Diagram of free energy changes and definitions for a concerted ET/bond rupture reaction.

where the partition functions Q refer to the cited species and contain all coordinates of $A_1^\bullet$, $B^\bullet$, and A_1B. The last two terms in eq 25 represent the free energy of reaction for $A_1B \rightarrow A_1^\bullet + B^\bullet$, the zero-point energies being included in the Q's.

We consider next, as in Figure 3, a free energy bookkeeping diagram for the concerted bond rupture/ET reaction, analogous to that in Figure 2. The left-hand portion of Figure 3 is the same as in Figure 2, but the right-hand part involves a termolecular collision of the products to form the encounter complex P. Depending on the detailed description of P, P may have a more or less linear or triangular configuration of A_1^-, $B^\bullet$, and $A_2^\bullet$. In the former case the six translations of the three products in the center of mass system of coordinates become two rotations and four "vibrations," all caged by the solvent molecules. In the triangular case there are either three rotations and three solvent-caged "vibrations" or, if two members of the three, e.g., A_1^- and $B_2^\bullet$, "rotate" about their own center of mass, there are four rotations and two vibrations in the motion of the three particles with respect to each other. We allow for each of these two possibilities, and one other, by using the symbol $q^{(2)}_{int}$ in Figure 3. In forming the termolecular encounter complex P from the three separated products, $q^{(6)}_{trans}$ is converted to $q^{(2)}_{rot}q^{(2)}_{vib}q^{(2)}_{int}$, where $q^{(2)}_{int}$ may denote $q^{(2)}_{vib}$, or $q^{(2)}_{rot}$, or $q^{(1)}_{vib}q^{(1)}_{rot}$. Further, some of the q_{rot}'s may be q_{hr}, where hr denotes a hindered rotation.

In Figure 3 we have again used the symbols $Q(0)$, $Q^\dagger$, and $Q(1)$, defined by stating that the partition function of the two reactants (in the center of mass system of coordinates) is $Q(0)$ $q^{(3)}_{trans}$, that of the TS is $Q^\dagger q^{(2)}_{rot}$ ($q^{(2)}_{rot}$ referring to the reactants in R), and that of the products is $Q(1)q^{(6)}_{trans}$. In Figure 3 it is seen that the partition functions of R and P are $Q(0)q^{(2)}_{rot}q^{(1)}_{vib}$ and $Q(1)$ $q^{(2)}_{rot}q^{(2)}_{vib}q^{(2)}_{int}$, respectively. The total number of coordinates in $Q(0)$ and $Q^\dagger$ is again three less than the total number of coordinates of the reactants, while $Q(1)$ has three less than $Q(0)$. We return to this point later. From the above definitions or Figure 3, the ΔG°_{RP} that enters into eq 7 is related to ΔG° by

$$\Delta G^\circ_{RP} = \Delta G^\circ + w_p - w_r + k_BT \ln[q^{(6)}_{trans}/q^{(2)}_{rot}q^{(2)}_{int}q^{(2)}_{vib}]_p/[q^{(3)}_{trans}/q^{(2)}_{rot}q^{(1)}_{vib}]_r \qquad (26)$$

where the p and r subscripts again denote the values in the P and R encounter complexes. For simplicity of notation we have written all q_{vib}'s in Figure 3 with the same symbol and all q_{rot}'s as being equal, but this notation is easily changed to specify the species to which each q refers.

The relation between ΔG°_{RP} and the E°'s, given below by eq 27, is obtained from eqs 25 and 26. We note that $Q_{A_1}Q_B/Q_{A_1B}$

can be written as $Q^{rv}_{A_1}Q^{rv}_{B}q^{(3)}_{trans}/Q^{rv}_{A_1B}$ where rv denotes the rotational−vibrational partition function.

$$\Delta G^\circ_{RP} = E^\circ_{A_2^{\bullet}/A_2^-} - E^\circ_{A_1^{\bullet}/A_1^-} + D_{A_1B} + w_p - w_r - k_BT \ln(Q^{rv}_{A_1^{\bullet}}Q^{rv}_{B^{\bullet}}q^{(2)}_{int}q^{(1)}_{vib}/Q^{rv}_{A_1B}) \quad (27)$$

The number of coordinates involved in the numerator of the partition function ratio in eq 27 is the same as the number in the denominator. We note that in the quantity ΔG°_{RP} the q_{trans}'s that were present in eq 26 have disappeared in 27, as expected. Further, when the attacking agent is $A_2^{\bullet-}$ in eq 4 instead of A_2^-, $E^\circ_{A_i/A_i^{\bullet-}}$ replaces $E^\circ_{A_i^{\bullet}/A_i^-}$.

For reaction 4 the free energy of formation of a system of specified X_1 and Y from the reactants A_1B and A_2^-, starting at the encounter complex R and not including the w_r or the partition function terms, is

$$\Delta G_r = \lambda_0 Y^2 + D_1(X_1 - 1)^2 \quad (28)$$

As a result of changes in X_1 by reaction, the encounter complex P, consisting of (A_1^-, $B^{\bullet}$, $A_2^{\bullet}$), is reached from R. For the corresponding free energy of formation of the system defined by (Y, X_1) from the products, starting from the configuration P, we have

$$\Delta G_p = \lambda_0(1 - Y)^2 + D_1 X_1^{\,2} \quad (29)$$

As before, λ_0 and $Q^\dagger$ can vary with position along the reaction coordinate.

Once again, the minimization should be of $\Delta G_r - k_BT \ln Q^\dagger$, subject to the constraint imposed by eq 7. However, to avoid introducing at this point variational parameters into $Q^\dagger$, we minimize ΔG_r subject to the constraint imposed by eq 7. We treat λ_0, as before, as more slowly varying than the other terms, and so λ_0 doesn't determine the Lagrangian multiplier but, as before, can depend on it, and thereby on $\Delta G^\circ_{RP}/\lambda$. We obtain

$$\Delta G^*_r = \frac{\lambda}{4}\left(1 + \frac{\Delta G^{\circ\prime}}{\lambda}\right)^2 \quad (30)$$

where λ now is given by

$$\lambda = \lambda_0 + D_{A_1B} \quad (31)$$

$\Delta G^{\circ\prime}$ is again given in terms of ΔG°_{RP} by the second half of eq 7, and ΔG°_{RP} is given by eq 27. We have

$$\Delta G^{\circ\prime} = E^\circ_{A_2^{\bullet}/A_2^-} - E^\circ_{A_1^{\bullet}/A_1^-} + D_{A_1B} + w_p - w_r - k_BT \ln q^{(2)}_{int}q^{(1)}_{vib} \quad (32)$$

after cancellations and setting $Q^{rv}_{A_1^{\bullet}}/Q^{rv}_{A_1^-} \cong Q^{rv}_{A_2^{\bullet}}/Q^{rv}_{A_2^-}$ (for eq 4a) or $\cong Q^{rv}_{A_2^{\bullet}}/Q^{rv}_{A_2^{\bullet-}}$ (for eq 4b).

We consider next the rate constant. Following the arguments that led to eq 15, we obtain

$$k_{ET} = Z[Q^\dagger/Q(0)] \exp(-\Delta G^*_{ET}/k_BT) \quad (33)$$

where Z is the relevant "collision frequency" between A_1B and A_2,[20b] ΔG^*_{ET} is given by

$$\Delta G^*_{ET} = w_r + \frac{\lambda}{4} + \frac{\Delta G^{\circ\prime}}{2} + \frac{\Delta G^{\circ\prime 2}}{4\lambda} \quad (34)$$

and λ is given by eq 31.

A question arises now concerning the factor $Q^\dagger/Q(0)$ in eq 33. The correct value of $Q^\dagger$ would again be obtained from a minimization procedure that included $-k_BT \ln Q^\dagger$ in the minimization. However, one simplifying approximation is to assume that the ET/bond rupture reaction is fully outer sphere and that $Q^\dagger/Q(0)$ equals the ratio of the large moment of inertia of the TS to that which appeared in R and hence in Z, and to suppose that the new rotations that may eventually appear in P (in $q^{(2)}_{int}$) are still, in the TS, the vibrations that they were in the reactants. In that case we have

$$k_{ET} = Z_{ET} \exp(-\Delta G^*_{ET}/k_BT) \quad (35)$$

where ΔG^*_{ET} is given by eq 34 and Z_{ET} contains[20b] a σ that is the distance between the centers of A_2^- and A_1B in the TS.

Although we shall not need it in the present analysis, the above comments are related to the rate constant of the back reaction to eq 4, which in turn is related to a termolecular "collision frequency" Z_{ter}: Following an argument similar to that which led to eq 15, Z_{ter} is $(k_BT/h)q^{(2)}_{rot}q^{(1)}_{vib}q^{(2)}_{int}/q^{(6)}_{trans}$, and so its value depends on the model assumed for the termolcular encounter complex P. Since the possibilities for $q^{(2)}_{int}$ can vary from $q^{(2)}_{rot}$ to $q^{(2)}_{vib}$, this Z_{ter} can vary by a couple of orders of magnitude, depending on the model used for P. Introducing values for $q^{(1)}_{rot}$ and $q^{(1)}_{vib}$, one finds[20c,d]

$$Z_{ter} \cong (\pi a^2)^{3/2}Z \quad (q^{(2)}_{int} = q^{(2)}_{vib}) \quad (36a)$$

or

$$Z_{ter} \cong 4\pi\sigma^2(\pi a^2)^{1/2}Z \quad (q^{(2)}_{int} = q^{(2)}_{rot}) \quad (36b)$$

where Z is the bimolecular collision frequency. Two of the a's in eq 36 are bending "vibrational" amplitudes, while one is a stretching amplitude, as is the one in eq 36b. The σ is on the order of several angstroms, and a is on the order of a tenth or a few tenths of an angstrom.

Equations 34 and 35 are equivalent to those derived for the concerted bond rupture/electron transfer derived earlier by Savéant[6] and also assumed in the work of Eberson.[23] The present description, which utilizes Figure 3, contains a more detailed discussion of the various free energy changes.

Unified Description and Effect of S_N2 Interaction on ET Rate. We consider next how, using eqs 5a and 13b, one can obtain a unified description for the reorganization energy for crossing the dotted line in Figure 1. The equation reduces in the appropriate limits to the S_N2 expression and to the concerted ET/bond rupture one. We then apply it to show how an incipient interaction of the S_N2 type could catalyze the outer sphere ET/bond rupture process.

We first note that when there is a pure outer sphere mechanism, i.e., no incipient S_N2 interaction, x_2 is so large that the X_2 in eqs 5 and 6 can be replaced by zero. One then obtains eqs 28 and 29, upon observing that the $\Delta G^{\circ\prime}$ for the S_N2 reaction, $\Delta G^{\circ\prime}_{SN2}$, equals $\Delta G^{\circ\prime}_{ET} - D_2$, where $\Delta G^{\circ\prime}_{ET}$ is the $\Delta G^{\circ\prime}$ for the ET reaction. Thus, eqs 28 and 29 for the ET reaction represent a special case of eqs 5 and 6, one where X_2 tends to zero. Similiar remarks apply to eq 34 for ΔG^*_{ET} being a special case ($X_2 = 0$) of eq 16, when one uses the above relation between the ΔG^*_{ET}'s and notes that β_{ij} becomes very small for the ET (large X_2) system.

We next consider how an S_N2-type interaction might catalyze an ET reaction, by reducing the reorganization energy barrier. The free energy surfaces $G_r(X_1,X_2,Y)$ and $G_p(X_1,X_2,Y)$ are equal on the TS dotted line in Figure 1a, for any given value of X_2.

We minimize ΔG_r in eq 5 with respect to X_1 and Y at a finite X_2, subject to the constraint in eq 7. We again introduce a Lagrangian multiplier, denoted now by m'. One finds $Y = -m'$, $X_1 = m'+1$, and $-(2m' + 1)\lambda_{ET} = \Delta G^{\circ\prime}_{ET} - 2D_2X_2$. The $\beta_{ij}(X_1,X_2)$ at this value of X_1 and X_2, given by eq 13b, is then subtracted, since this β_{ij} is resonance energy at the crossing of the two surfaces at the given X_2. In this way we obtain the barrier for an ET reaction at a finite X_2:

$$\Delta G_r^{\ddagger}(X_2) - \beta_{ij}(X_2) = \Delta G_r^{\ddagger}(X_2{=}0) - D_2X_2(1 + \Delta G^{\circ\prime}_{ET}/\lambda_{ET}) + D_2X_2^2\lambda_{S_N2}/\lambda_{ET} - (\gamma_1 D_1'\gamma_2 D_2')^{1/2}\{2X_2[1 - (\Delta G^{\circ\prime}_{ET} - 2X_2D_2)/\lambda_{ET}]\}^{1/2} \quad (37a)$$

where we note that $\beta_{ij}(X_2{=}0) = 0$ and that $\lambda_{S_N2} = \lambda_{ET} + D_2$, and so $\Delta G^{\circ\prime}_{S_N2} + \lambda_{S_N2} = \Delta G^{\circ\prime}_{ET} + \lambda_{ET}$.

At small X_2, the X_2^2 term in eq 37a can be neglected, and since $1 + \Delta G^{\circ\prime}_{ET}/\lambda_{ET}$ is positive (except in any "inverted" region), the second term in eq 37a leads to a lowering of the ET free energy barrier, as does the last term. This lowering is due to the presence of X_2, i.e., to the proximity of $B^{\bullet}$ to A_2^-. The possibility of there being some S_N2-like interaction in an ET reaction has been suggested earlier.[1c,16] In eq 37a there are two effects of this nature.

The value of X_2 that causes the maximum lowering of the ET barrier is the value at the S_N2 TS: Minimization of the second term in the right side of eq 37a shows this X_2 to be $^1/_2(\lambda_{S_N2} + \Delta G^{\circ\prime}_{S_N2})/\lambda_{S_N2}$. However, such an X_2 would lead to the S_N2 reaction 3 rather than to the ET reaction 4.

To calculate the reaction rate using eq 37a, it is necessary to have an expression for the ratio of the partition function of the TS to that of the reactants. (There is also, for the ET case, some decision to be made for the $q_{int}^{(2)}$ in eq 32 for ΔG°_{RP}.) Examples of this partition function ratio were given above for the two limiting cases. In general, as in all applications of TS reaction rate theory, some estimate must be made for the behavior of the coordinates in the TS, namely whether they are vibrations, hindered rotations, or rotations, based on a description of the relevant parts of the potential energy surface for the solute in the TS. Equations 20 and 35 are limiting cases. When most trajectories cross the TS, instead, in some region between those two paths (arrows in Figure 1a), the three coordinates giving rise to the q_{vib}^3 in eq 20 may be, instead, hindered rotations, and we simply write the partition function as $q_{int}^3(X_2)$. The latter reduce to q_{vib}^3 for the pure S_N2 path and to q_{rot}^3 for the pure ET/bond rupture path. We have

$$k = Z(q_{int}(X_2)/q_{rot})^3 \exp([-\Delta G_r^{\ddagger}(X_2) + \beta_{ij}(X_2)]/k_BT) \quad (37b)$$

where $\Delta G_r^{\ddagger}(X_2) - \beta_{ij}(X_2)$ is given by eq 37a. The Z is also a function of X_2, a relatively weak one, ranging from Z_{S_N2} at $X_2 \approx 1/2$ to Z_{ET} at $X_2 \approx 0$. The appropriate value of X_2 in eq 37b is obtained by maximizing ln k with respect to X_2. Equation 37b for k yields the appropriate limits of eqs 20 and 35.

The X_2 effect, i.e., a large enough X_2 that reduces the ET barrier but not so large that the reaction would become mainly S_N2, has implications for a $\Delta H^{\dagger}$ and $\Delta S^{\dagger}$ correlation. These quantities are obtained from $\Delta G^{\dagger}$ using the standard thermodynamic expressions. We use X_2 as a variational parameter. The $\Delta H^{\dagger}(X_2)$ and $\Delta S^{\dagger}(X_2)$ vary in opposite directions with X_2 as one moves from large A_iB distances [large $\Delta H^{\dagger}(X_2)$ and a less negative $\Delta S^{\dagger}(X_2)$] to smaller A_iB distances (smaller $\Delta H^{\dagger}$ and more negative $\Delta S^{\dagger}$) along the dotted line. For any reaction the most important crossings of the TS hypersurface are those that occur at the minimum (or minima) of $\Delta G^{\dagger}(X_2)$, i.e., at $\partial[\Delta H^{\dagger}(X_2) - T\Delta S^{\dagger}(X_2)]/\partial X_2 = 0$ along the dotted line. Thereby, a suitable variational transition state theory would yield the value (unimodal case) or values (bimodal case) of X_2 and hence of $\Delta S^{\dagger}(X_2)$ and $\Delta H^{\dagger}(X_2)$. When most of the flux density passage occurs in the ET path region, it would yield the most probable value of X_2 for catalyzing the ET reaction. The $\Delta H^{\dagger}(X_2) - T\Delta S^{\dagger}(X_2)$ function provides insights into the question of unimodality *vs* bimodality of the flux density for crossing the dotted line (TS).

III. Applications and Discussion

We consider several applications of the above expressions in this section: (i) relation of self-exchange and cross S_N2 reactions, (ii) relation between ET and S_N2 rate constants, (iii) entropies of activation of the two reactions, (iv) effect of driving force on the rate constant, and the topic of linearity of ln k_{rate} *vs* E° plots. We also consider a number of other topics including numerical results, some remarks on computer simulations, and nonequilibrium polarization.

Cross-Relation for Rate Constants. The identity reactions corresponding to the "cross-reaction" 3 are

$$A_1 - B + A_1^- \rightarrow A_1^- + BA_1 \quad (38)$$

$$A_2 - B + A_2^- \rightarrow A_2^- + BA_2 \quad (39)$$

From eqs 12, 13, 16, and 20 for the S_N2 reaction, it follows approximately that the rate constants of the cross-reaction 3 and the identity reactions 38 and 39 are related by

$$k^{12}_{S_N2} \cong (k^{11}_{S_N2}k^{22}_{S_N2}K^{12}_{S_N2})^{1/2} \quad (40)$$

when the difference of square roots in eq 13d, and the quadratic terms in eqs 13d and 16, can be neglected. In eq 40 the 12 superscript refers to the cross-reaction 3, and 11 and 22 refer to the self-exchange reactions 38 and 39, while $K^{12}_{S_N2}$ refers to the equilibrium constant of reaction 3.

If the quadratic terms in eq 13d and 16 are included, an additional factor enters into eq 40, just as an extra factor occurs in the cross-relation for ET reactions.[19] Equation 40 has been tested for various reactions,[1c] methyl radical transfers for example, with A_1 and A_2 being arylsulfonates (no charge transfer),[5] and has been tested with various quantum chemistry calculations (with an additional quadratic term included, though it is often small).[24] When eq 40 is fulfilled for S_N2 reactions, it suffices in any analytical or numerical calculations to focus only on the identity reactions 38 and 39, a considerable simplification. It also serves to distinguish between thermodynamic and kinetic (or "intrinsic"[7b]) effects on the energy barrier. Also, there is the well-known advantage that an interpretation or understanding of N identity reactions then provides one of the $N(N - 1)/2$ S_N2 cross-reactions.

Relation of ET and S_N2 Rate Constants. In experiments the reactions between aromatic radical anions and alkyl or other halides have been extensively studied and have frequently been assumed to have ET rather than S_N2 mechanisms. For appreciably sterically hindered RX's the absence of inversion has been confirmed,[25] while in others inversion is a variable component.[8,9] The rates of such reactions, e.g., of eqs 1a or 1b, have been compared with those whose S_N2 character is uncertain, but which have the same E° for the attacking anion A_2^-, for a given RX. That is, A_2^- is different for the two reactions, but its E° is the same. When the rate constants are comparable, it has then frequently been presumed that the tested reaction is of the ET-type, eq 1, rather than S_N2, reaction 2. For rate constants k_{ET} of reactions of aromatic anion radicals

with *tert*-alkyl halides, Savéant obtained excellent agreement between the experimental data and his equations (the present eqs 31, 34, and 35) and quite good agreement for other (*n*- and *sec*-) alkyl halides,[16] the experimental barrier now being roughtly 0.1 eV lower than the calculated value, perhaps reflecting some S_N2-like interaction that catalyzes the ET/bond rupture reaction and, in addition, some S_N2 reaction path.

In the experiments of Lund and co-workers[3,26] the reactions of a carbanion, the enolate anion of 4-methoxycarbonyl-1-methyl-1,4-dihydropyridine ($\mathbf{I}^-$ below) have been studied and compared with the attack of the same RX by an aromatic radical anion of the same $E°$. The D_{A_2B} appearing in all the equations is the presently unknown dissociation energy of the reaction $\mathbf{I}R \rightarrow \mathbf{I}^\bullet + R$:

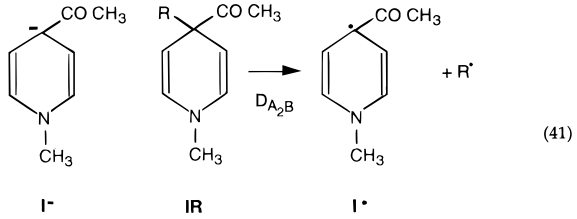

(41)

The experiments were performed with R's such as admantyl, neopentyl, *tert*-butyl, *sec*-butyl, *n*-butyl, and ethyl. In reactions with sterically hindered alkyl halides the *k*'s were similar to those with aromatic radical anions of the same $E°$'s,[3b] suggesting thereby an outer sphere ET mechanism for those reactions of $\mathbf{I}^-$. The stabilization of the TS was large, on the other hand, for the least hindered systems. For example, for the ethyl bromide system, the ratio of rate constants k_{S_N2}/k_{ET} was about 2500.[3b]

We compare the expressions for k_{S_N2} and k_{ET}, using for brevity the two-interacting-states S_N2 model, and consider reactions with the same A_1B but with different A_2's having the same $E°$. From the equations for S_N2 reactions and those for ET reactions we obtain, in the linear expansion ($|\Delta G°'_{RP}|/\lambda \ll 1$) regime,

$$\frac{k_{S_N2}}{k_{ET}} \cong \frac{Z_{S_N2}}{Z_{ET}}\left(\frac{q_{vib}}{q_{rot}}\right)^3 \exp\left(\frac{\lambda_0^{ET} - \lambda_0^{S_N2}}{4k_BT} + \frac{D_{A_2B}}{4k_BT} + \frac{(\gamma_1 D'_{A_1B}\gamma_2 D'_{A_2B})^{1/2}}{k_BT}\right) \quad (42)$$

using eq 13c and so not using the approximation of neglecting the difference of square root terms in eq 13d. (If the two $\gamma_i D'_i$'s differ considerably, the approximation of replacing their geometric mean by an arithmetic one becomes poor.)

It may also be necessary to include in some cases the quadratic terms that were present in eqs 16 and 34. In that case there will be, as noted earlier, additional factors, on the right side of eq 42, when the $|\Delta G°'|/\lambda$'s becomes appreciable. The $\lambda_0^{ET} - \lambda_0^{S_N2}$ in eq 42 is expected to be positive, because of the larger charge separation in the TS of the ET reaction. To interpret the data in ref 3a, the energy exponent in the ratio k_{S_N2}/k_{ET} would need to be only about 5 kcal mol^{-1}. On the other hand, in a Finklestein reaction,[23,3b] $I^- + n\text{-BuBr} \rightarrow n\text{-BuI} + Br^-$, the ratio of k_{S_N2}/k_{ET} is estimated to be 4×10^{20}, which corresponds to a difference in free energy barrier of 29 kcal mol^{-1}. In the next section we estimate the pre-exponential factor in eq 42 to be about $10^{11}/10^9$, i.e., about 100.

Savéant and co-workers[2b,c,15] studied the S_N2 reaction of Fe("0") and Fe(I) porphyrins, prepared electrochemically, with RX, where various alkyls were chosen for R.

$$Fe(\text{“0”}) + RX \rightarrow Fe^{II}R^- + X^- \quad (43)$$

$$Fe(I) + RX \rightarrow Fe^{III}R^- + X^- \quad (44)$$

They also studied the ET reactions between RX and aromatic anion radicals. When the alkyl group in R was not sterically hindered, the S_N2 reaction of the Fe porphyrins with RX was faster than the ET reaction by approximately 2 orders of magnitude: The log *k* *vs* the $E°$ curve of the electron donor (the Fe porphyrin or the aromatic anion radical) was roughly parallel to that for the aromatic anion radical. To further test eq 42 for k_{S_N2}/k_{ET} adequately, it will be necessary to know or estimate the dissociation energy of the $Fe^{II}R^-$ or $Fe^{III}R^-$ bond in eqs 43 and 44 and to make some estimate of the γ_i's and D'_i's. In a later section we make some estimates for other reactions.

In the above data in ref 15 the difference in the relevant $E°$'s was zero, and so if D_{A_2B} is approximately constant for different $Fe^{II}R^-$'s (i.e., different B's in reaction 3) which do not involve sterically hindered alkyl's, then the vertical difference of the two ln *k* *vs* $E°$ plots should be constant (upon neglecting the quadratic term). The constant vertical difference in the plot indicates, as Savéant and co-workers have noted,[15] that D_{A_2B} is approximately independent of B, for B's that do not cause steric hindrance. They also noted that there are the two opposing effects influencing the k_{S_N2}/k_{ET} ratio: (1) a more restricted transition state for the S_N2 reaction and (2) a lowered energy activation for S_N2, because of the bond formation. The two effects are present in eq 42.

An analogous study is that by Walder,[27] who studied an S_N2 reaction between the cobalt(I) form of vitamin B_{12} and various alkyl halides: *n*-butyl iodide, bromide and chloride, ethyl bromide, and benzyl chloride.

$$Co^I + RX \rightarrow Co^{II}R + X^- \quad (45)$$

For these various halides the *k* of the S_N2 reaction was a couple of orders of magnitude faster than its ET counterpart (aromatic anion of the same $E°$).[27] If the $D_{Co^{II}-R}$ is approximately independent of R, such a parallelism is consistent with eq 42, and once again a knowledge of $D_{Co^{II}-R}$ and of γ_i and D'_i in eq 13 would be helpful.

Another comparison of interest is the ratio of k_{S_N2}/k_{ET} when the A_1 in reactions 3 and 4 is varied at fixed A_2^- and B. From the equations for ET reactions and for S_N2 reactions we again obtain eq 42. Experimentally, in the reaction of anthracene anion radicals with 2-octyl halides the ratio of inversion/racemization (and so k_{S_N2}/k_{ET}) follows the order Cl > Br > I[8] and in the same order for the reaction of anthracene radical anions with methyl halides.[9] This order is the one expected from eq 42 from the relative bond strengths D_{RX} and (for a choice $D'_i = D_i$) the γ_i discussed later. The contribution of the S_N2 mechanism for the 2-octyl halides was[8] 5, 8, and 11%, and for the methyl halides it was[9] 25, 77, and 97% for RI, RBr, and RCl, respectively.

Entropies of Activation. We consider next the entropy of activation $\Delta S^\dagger$ obtained from the transition state theory expression:[20a]

$$k = \frac{k_BT}{h}e^{-\Delta G^\dagger/k_BT} = \frac{k_BT}{h}e^{-\Delta H^\dagger/k_BT}e^{-\Delta S^\dagger/k_B} \quad (46)$$

where $\Delta H^\dagger$ and $\Delta S^\dagger$ are, in turn, obtained from the thermodynamic expressions $\Delta H^\dagger = \partial(\Delta G^\dagger/T)/\partial(1/T)$ and $\Delta S^\dagger = -\partial\Delta G^\dagger/\partial T$. Thereby,

$$\Delta H^{\dagger} = -k_B \frac{\partial\, ln(k/T)}{\partial(1/T)} = E_a - k_B T \qquad (47)$$

and

$$\Delta S^{\dagger}/k_B = \ln(kh/k_B Te) + E_a/T \qquad (48)$$

since the activation energy E_a is defined by $-k_B\, \partial\, ln\, k/\partial(1/T)$. Equation 48 was used by Lund and co-workers[3] to obtain $\Delta S^{\dagger}$.

We next use results from some gas phase S_N2 reactions to estimate the pre-exponential factor in eq 20. For such a reaction when $\Delta S^{\circ} \cong 0$, we can write $k \cong Z(q_{vib}/q_{rot})^3 \exp(-\Delta U/k_B T)$, where ΔU is a term essentially independent of temperature. We write this k as $C'(T) \exp(-\Delta U/k_B T)$. When $C'(T)$ varies as T^n and the rate constant k is also written as $A \exp(-E_a/k_B T)$, with E_a defined as above, it follows that $A = C'(T)e^n$. We now apply this expression to gas phase reactions, so as to estimate $Z_{S_N2}(q_{vib}/q_{rot})^3$ from data on those reactions.

Typical pre-exponential factors, A, for bimolecular metathesis reactions (tight TS) involving polyatomic species, e.g., $CH_3^{\bullet} + HR \rightarrow CH_4 + R^{\bullet}$, are[28] about $10^{8.6}$ M^{-1} s^{-1}. Since q_{rot} varies as $T^{1/2}$ while Z_{S_N2} varies as $T^{1/2}$, n is then -1, if q_{vib} is roughly unity. Then $C'(T)$, which equals Ae^{-n}, is about 10^9 M^{-1} s^{-1}, and we note that $C(T)$ is $Z_{S_N2}(q_{vib}/q_{rot})^3$. If for a loose TS reaction the pre-exponential factor in eq 35, Z_{ET}, is about 10^{11} M^{-1} s^{-1}, the ratio of the pre-exponential factors in eq 42 has the value of about 100, as mentioned in the previous section.

We turn next to the $\Delta S^{\dagger}$ in eq 48. When we write the k in eq 20 or 35 in the form $k = C(T)\exp(-\Delta G^*/k_B T)$, with $C(T) \propto T^n$, it then follows from the definition of E_a that $E_a = \Delta H^* + nk_B T$, where $\Delta H^* = \partial(\Delta G^*/T)/\partial(1/T)$, and that

$$\Delta S^{\dagger} = \Delta S^* + k_B \ln(C(T)h/k_B T) + (n-1)k_B \qquad (49)$$

where $\Delta S^* = -\partial \Delta G^*/\partial T$.

When the dependence of the λ on T is neglected (the dependence is expected to be weak, as in the usual ET's) and the quadratic term in eq 34 is neglected, eq 49 yields for an ET reaction

$$\Delta S^{\dagger}_{ET} = k_B \ln(Z_{ET}h/k_B T) - \frac{1}{2}k_B - \frac{\partial}{\partial T}(E^{\circ}_{A_2^{\bullet}/A_2^-} - E^{\circ}_{A_1^{\bullet}/A_1^-}) - \frac{1}{2}\frac{\partial}{\partial T}(w_r + w_p) \quad \text{(ET, loose TS, linear expansion)} \qquad (50)$$

upon using eqs 34 and 35 and, for the moment, neglecting any entropy change associated with the partition function terms in eqs 32. We return to that point later.

Similarly for the SN2 reaction, using the term linear in $\Delta G^{\circ\prime}$ in eq 16 and neglecting any dependence of λ on temperature, eqs 20 and 49 yield

$$\Delta S^{\dagger}_{S_N2} = \left[k_B \ln Z_{S_N2}\left(\frac{q_{vib}}{q_{rot}}\right)^3 \frac{h}{k_B T}\right] - 2k_B + \ldots - \frac{1}{2}\frac{\partial}{\partial T}(E^{\circ}_{A_2^{\bullet}/A_2^-} - E^{\circ}_{A_1^{\bullet}/A_1^-}) - \frac{1}{2}\frac{\partial}{\partial T}(w_r + w_p) \quad \text{(tight TS, linear expansion)} \qquad (51)$$

From eq 51, apart from the $\partial E^{\circ}/\partial T$ term, which is largely related to any entropy change associated with the solvation change from A_2^- to A_1^-, if we neglect the $\partial w/\partial T$ terms, which are expected to be minor unless both reactants are charged, then from $Z_{ET} \cong 10^{11}$ M^{-1} s^{-1} one obtains $\Delta S^{\dagger}_{ET} \cong -9.5$ eu. Instead, from eq 51 and the above value, 10^9 M^{-1} s^{-1}, for $Z_{S_N2}(q_{vib}/q_{rot})^3$, eq 51 yields $\Delta S^{\dagger}_{S_N2} \cong -22$ eu. We next compare these results for the ET and S_N2 reactions with the data.

In ref 3 the least negative $\Delta S^{\dagger}$ for the ET reactions was about -9 eu, (in some cases 1−2 eu less) and the most negative $\Delta S^{\dagger}$'s for SN2 reactions involving I^- were about -22 eu. These results agree with the above estimates. It would be helpful helpful to have direct data on the $\partial \Delta E^{\circ}/\partial T$ term in eqs 50 and 51 to see how small it is.

However, many of the largely ET/bond rupture reactions in ref 3 have a $\Delta S^{\dagger}$ that is intermediate in value between the values of -9 and -22 eu. For example, the reaction between an anthracene radical anion and *n*-butyl bromide was investigated over a very wide range of temperatures, -50 to 50 °C and for a number of other reactions, and showed a $\Delta S^{\dagger}$ of -16 eu. The $\Delta S^{\dagger}$ for the reaction with *sec*-butyl bromide and with a number of other halides also had about that value. If we can neglect the $d\Delta E^{\circ}/dT$ due to an approximate cancellation of anion solvation effects, then this $\Delta S^{\dagger}$ may reflect steric effects and another factor mentioned later.

The details of the temperature dependence of the ratio of inversion/racemization, i.e., of k_{S_N2}/k_{ET}, are of particular interest: From the study of the ratios for the reaction of anthracene anion radicals with 2-octylhalides (X = Cl, Br, I) at 25 °C and at −50 °C, one can estimate from the data[8] that the difference in activation energies of the ET and S_N2 reactions is between 1.6 and 2.9 kcal mol^{-1}, instead of the 5 kcal mol^{-1} mentioned above for a different system. The ratio of pre-exponential factors was between *ca.* 1 and 15, instead of being about 100 or more. In this case a bimodal characterization of the ratio of yields of S_N2 and ET mechanisms seems less attractive than a unimodal one, in which the ratio of fluxes ending up as S_N2 or as ET products would be somewhat energy-dependent though presumably not as much as in the bimodal case. In the following we consider first a choice $D_i' \equiv D_i$. Elsewhere, to compare with an impressive correlation of Pellerite and Brauman (ref 12, 1983), we consider instead a different choice, one involving E_{A_i}.

Another consequence of a unimodal flux density is a possible continuous correlation between $\Delta H^{\dagger}$ and $\Delta S^{\dagger}$ over the above range of $\Delta S^{\dagger}$'s within a series of related compounds. We have already noted the limiting situations, often referred to in the literature, of a pure S_N2 reaction having a very negative $\Delta S^{\dagger}$ and a relatively low $\Delta H^{\dagger}$, and a pure outer sphere ET reaction having a much less negative $\Delta S^{\dagger}$ and a relatively high $\Delta H^{\dagger}$. Along the TS dotted line in Figure 1 between the ET and S_N2 arrows one expects the potential energy to decrease steadily as one moves from the region where the A_iB distances are large, partly because the splitting of the two surfaces is increasing and partly because one is also entering a more bonding region. Only around the S_N2 arrow is a saddle-point expected to appear.

If the flux density is unimodal, and if one characterizes the various regions of the dotted line in Figure 1a (and more generally of the TS hypersurface) with some parameter, such as X_2, the opposite trends of $\Delta H^{\dagger}$ and $\Delta S^{\dagger}$ with X_2 described earlier would lead to a smooth correlation between the two for a given reaction series. In particular, it seems to occur in the reaction of the $\mathbf{I}^-$ in eq 41 with alkyl bromides,[3a] but thus far there appear to be only three sets of points on the line, two with $\Delta S^{\dagger} \approx -21$ to -22, two with $\Delta S^{\dagger} = -16$, and two with $\Delta S^{\dagger} = -9$ to -9.5 eu. The $\Delta S^{\dagger}$ for reacting RBr's range from those for unhindered (-22 to -22 eu) to semihindered (-16 eu) to hindered (-9 to -9.5 eu). It would be instructive to see if experimental points can be obtained between the above three sets.

A related aspect of this temperature or $\Delta S^{\dagger}$ behavior concerns the linearity of the ln k *vs* $1/T$ plot mentioned earlier for the reaction between anthracene radical anions and *n*-butyl bromide

over the wide temperature range of −50 to 50 °C.[26a] There was no indication of a possible change of mechanism, i.e., no change of slope, from a S_N2 low pre-exponential factor/low activation energy behavior at low temperatures to a higher ET pre-exponential factor/higher activation energy behavior at high temperature.[3] The result is consistent with that described in the previous section on the inversion/racemization ratio for the reaction of anthracene radical anions with optically active 2-octyl halides (namely, having an intermediate value of the ratios of pre-exponential factors and of the difference of activation energies). These results, too, seem to favor a unimodal description of the flux density. However, a more detailed analysis is needed, preferably supported with trajectories on a realistic potential energy surface.

We conclude this section with some remarks on the entropy term associated with the $\Delta G^{\circ\prime}$ appearing in eq 32 and which would make a contribution $^1/_2\Delta S^{\circ\prime}$ to the entropy of activation $\Delta S^{\dagger}$ in the linear regime ($\Delta S^{\circ\prime} = -\partial\Delta G^{\circ\prime}/\partial T$). The difference of E°'s contributes to $\Delta S^{\circ\prime}$ a component principally related to the solvation entropy of the product ion A_1^- minus that of A_2^-. If the $q_{int}^{(2)}$ in 32 is largely $q_{vib}^{(2)}$, with small amplitudes, as we have tacitly assumed in writing eq 50, then the last partition function term in 32 will make relatively little contribution to $\Delta S^{\circ\prime}$. If, however, the $q_{int}^{(2)}$ is $q_{rot}^{(2)}$ or involves very floppy hindered rotations, then the term will contribute a positive contribution to $\Delta S^{\circ\prime}$ and hence to $\Delta S^{\dagger}$. The idea that developing rotations might contribute to $\Delta S^{\dagger}$ was suggested by Savéant.[29] It would be very useful to determine the $\Delta S^{\circ\prime}$ of some of the reactions, so that its role in affecting $\Delta S^{\dagger}$ could be studied more closely.

Effect of Driving Force, $-\Delta G^\circ$. There have been many studies of the effect of driving force, or more specifically of the effect of the E° of the reactant A_2^- in eq 4, on log k_{ET}. Such plots are meaningful if the λ in eq 34 does not change with A_2^-. Similar remarks apply to the the S_N2 reaction 3.[2c] In this sense, eq 40 is more general than any relation that does not allow for any differences in $k_{S_N2}^{22}$ (and thereby in λ) in a reaction series where A_2^- is varied.

Typically, the slopes of the $-k_BT \ln k$ *vs* E° plots of the ET reactions have been near the expected value of 0.5, or less,[1d,3,16,26] because the reaction is estimated to be typically downhill. One puzzle, or apparent puzzle, has been the behavior of the $\ln k_{ET}$ *vs* E° plot for the reaction of aromatic anion radicals with *tert*-butyl bromide. It is linear rather than being curved (parabolic equation) over a substantially larger range of E°'s than was expected.[3a] A pre-exponential factor of 5×10^{12} M^{-1} s^{-1} and λ of 90 kcal mol^{-1} were used to calculate the expected parabolic relation, but even if a factor of 10^{11} M^{-1} s^{-1} and (to yield the same rate constant) the larger λ of 100 kcal mol were used, a linear behavior would still be surprising. Curved plots are well-known in the literature for other systems, for example for $Fe(cp)_2^{+/0}$ undergoing long-range ET across an adsorbed alkanethiol monolayer to an electrode[30] and in various homogenous reactions.

There are two views[3a,16] in the literature on the significance of this linearity or apparent linearity for the above reaction, in part because the data at the high-*k* end of the plot were obtained by a different method from the others. We also note that the $\Delta S^{\dagger}$ data indicate a mainly (or entirely) outer sphere ET mechanism, but the experimental $\Delta S^{\dagger}$ seems to become somewhat less negative at the lower *k* end.[26a] (Data on at the high-*k* end do not appear to be available.) If this effect is real, it could contribute to the unexpectedly high values at the low-*k* end, though not enough, a factor of 7 instead of the 100 expected from a quadratic relation, eq 34. It would be helpful to know, if the S_N2 products are measurable, how the ratio of S_N2/ET products changes over the large range of E°'s studied. This reaction of aromatic anion radicals with *tert*-butyl bromide is one where very little S_N2 contribution is expected.

As noted above, there is some controversy concerning the legitimacy of plotting the high-*k* points on the same plot as the others. Should the points prove to be legitimate, then the remarks made on q_{int}^2 at the end of the preceding section indicate that the pre-exponential factor would be higher than that expected from eq 35, which does not take into account some consequences of the A_1B bond extension. It would be useful to attempt to measure the $\Delta S^{\dagger}$ at the high-*k* end, to see if it is indeed less negative than in the middle-*k* region.

Comparison of the Numerical Results and the S_N2 Model. In comparing eqs 11 and 12 for the two-interacting-states model for the S_N2 reaction with some numerical results, we focus first on the identity reactions, for which $\Delta G^{\circ\prime}$ vanishes.

We compare the S_N2 model with data on gas phase and solution phase S_N2 reactions, initially for the group VII members of the periodic table. For the identity reaction $A_iB + A_i^- \rightarrow A_i^- + BA_i$, when B is CH_3 and A_i^- is F^-, Cl^-, Br^-, and I^-, the solution phase barrier is[1c,4d] about 32, 27, 24, and 22 kcal mol^{-1}, respectively, while the gas phase barrier is 13(?), 10, 11 and 6(?) kcal mol^{-1}.[12,4d] (These gas phase barriers are from the bottom of the close contact ion−dipole well to the barrier maximum.[4d]) The differences are 19(?), 17, 13, and 16(?) kcal mol^{-1}, respectively. In the two-state model this difference is $\lambda_0/4$, the λ_0 being evaluated at the TS geometry. An independent measure of a related quantity, the single-ion vertical reorganization energy, denoted by $\lambda_0(A_i^-)$, is available[22] from threshold energies of photoelectron emission by ions in solution, using eq 21. From the data[22] for F^-, Cl^-, Br^-, and I^-, $\lambda_0(A_i^-)/4$ is estimated to be 14, 10, 9, and 8 kcal mol^{-1}, respectively. One expects the $\lambda_0/4$ for the $A_i^- + CH_3A_i$ identity reaction to be between 1 and 2 times $\lambda_0(A_i^-)/4$. The values cited above are roughly consistent with this expectation.

We turn next to the barrier for the gas phase identity reactions, which is $(0.5 - \gamma_i)D_{A_iB}$, according to eq 16. The ratio of the experimental gas phase barriers[12,4d] to D_{A_iB}'s [4d] is 0.12(?), 0.12, 0.15, and 0.11(?) for $A_i^- = F^-$, Cl^-, Br^-, and I^-, respectively. Thus, the two-state model leads to a $\gamma_i \cong 0.38$, so indicating a very large effect of the "resonance" interaction of the (multi) states to lowering the energy barrier. The ratio of the experimental gas phase barrier to the D_{A_iB} for these reactions $(0.5 - \gamma_i)$ is seen to be on the same order (∼10%) as for reactions involving neutrals.

Applying next the above arguments to S_N2 reactions in solution, if we assume that the barrier is *ca.* $1.5\ \lambda_0(A_i^-)/4 + 0.12D_{A_iB}$, we obtain 34, 25, 22, and 19 kcal mol^{-1} for the F^-, Cl^-, Br^-, and I^- reactions. These values are, as expected from the choice of the two parameters, close to the experimental values of about 32, 27, 24, and 22 kcal mol^{-1}.

We consider next some A_i^-'s, such as OH^- and CN^-, described[4e] as being poor leaving groups. (It has been pointed out[4] that terms such as leaving group ability and nucleophilicity are replaced, in the language of ref 7b and 11, by other terms: intrinsic barrier, thermodynamic driving force.) The attacking atoms are members of groups IV−VI in the periodic table, instead of the halide group VII. The halides tend to have lower barriers relative to the dissociation energies. For example, for CH_3O^-, NC^- (C attack), $CH_3CO_2^-$, CH_3S^-, and HCC^-, the ratio of experimental gas phase barriers to D_{A_iB} is (roughly) 0.35, 0.29, 0.18, 0.32, and 0.35, respectively. Each of these ratios is substantially higher than the average value for the halides. The γ_i defined by eq 13 is seen to be 0.15, 0.21, 0.32,

0.18, and 0.15, respectively, values that on the average are much smaller than the 0.38 average for the halides. (The $CH_3CO_2^-$, with its more delocalized electronic structure, may be a special case.)

We consider next some reactions in solution for which there are data on and D_{A_iB} and $\lambda_0(A_i^-)$. For OH^- we estimate the value of $\lambda_0(A_i^-)$ from photoelectron emission threshold energies[22] to be 37 kcal mol^{-1}. For CN^- the $\lambda_0(A_i^-)$ estimated from data on charge transfer spectra,[22c] using the correlation[22a] between them and threshold energies, is about 44 kcal mol^{-1}. In the two-interacting-state model if one had assumed $1.5\ \lambda_0(A_i^-)/4 + 0.12D_{A_1B}$, the calculated barriers would be 24 and ~30 kcal mol^{-1}, which are much lower than the observed values of 42 and 51.[4d] Thus, the parameter γ_i again has a value for these non-halide systems that is smaller than that for the halides. A γ_i of 0.16 instead of 0.38 yields 45 and 50 kcal mol^{-1} for the OH^- and CN^- reactions, respectively, which are close to the observed 42 and 51.

We consider next some cross-reactions, using eq 42 but recognizing that the higher terms would be needed when a $\Delta G^{\circ\prime}$, either for S_N2 or ET or both, becomes appreciable. The Finkelstein reaction, $X^- + CH_3Y \rightarrow X\,CH_3 + Y^-$, has, as noted earlier an extremely high ratio of k_{S_N2}/k_{ET}, ~10^{20}. There appear to be three contributions to this effect: (i) The D_{A_2B}'s are large for the alkyl halides, leading to a large stabilization of the S_N2 product. (ii) The comparison of the S_N2 reactions is with reactions of aromatic radical anions, of the same E°, instead of halide ions. The aromatic anions contribute a substantially smaller amount than halide ions to $\lambda_0/4$. The λ_0 for the self-exchange reactions of aromatic ions self-exchange reactions has been estimated[10,2b] to be about 15 kcal mol^{-1}, corresponding to about 7.5 kcal mol^{-1} for a single ion, while the single ion λ_0's for the halides estimated from the solution photoelectron emission threshold energies[22] ion data are 56, 40, 36, and 32 kcal mol^{-1}, respectively. (iii) From the gas phase barriers for the identity reactions for $X^- + CH_3X \rightarrow XCH_3 + X^-$, the γ_i was estimated above to be very large when X^- is a halide, namely, 0.38. This large γ_i for the halides leads to a considerable reduction of the energy barrier in a two-state model.

We consider next the reactions between $\mathbf{I}^-$ and RX, compared with the aromatic anion radical−RX reaction. The k_{S_N2}/k_{ET} ratio was considerably less than in the above Finkelstein reaction case. A reason is the (probably) much smaller bond energy and γ_i of **I**R, as compared with the halide−R bonds formed in the Finkelstein reaction. The λ_0 was also more favorable to ET than in the preceding case, since now an aromatic anion radical is the attacking agent for *both* reactions.

In the case of the Fe("0"), Fe(I), and Co^I attacking agents, in reactions 41−43, the $Fe^{II}R^-$, $Fe^{III}R^-$, and $Co^{II}R$ bonds are presumably stronger than the AR• bonds, where A is an aromatic group, since k_{S_N2}/k_{ET} is substantially larger than unity. Turning next to the reaction of aromatic anion radicals with the *s*-octyl halides, their k_{S_N2}/k_{ET} ratio is less than 1. Presumably this newly formed AR• bond in the S_N2 reaction is weaker than the one with these metal groups.

Quantum Chemistry Calculations and γ_i. We have summarized in the preceding section some values of the ratio of the experimental energy barriers of gas phase S_N2 identity reactions to dissociation energies. From them typical values of γ_i can be obtained for the different groups in the periodic table. In some quantum chemistry calculations of Wolfe *et al.*[24a] the ratio of the calculated energy barrier[24a] to the experimental dissociation energy[4d] for H^-, HCC^-, NC^- (C attack), CH_3O^-, HO^-, HOO^-, and HS^- is 0.55, 0.43, 0.36, 0.29, 0.23, 0.26, and 0.21, respectively, while those for the halides F^- and Cl^- are 0.11 and 0.065. Once again there is a considerable difference between the A_i^-'s of group VII on one hand and those of groups IV and VI on the other, and even a significant difference between groups IV and VI. The values of γ_i for the members of groups IV−VI, obtained by equating the above ratios to $0.5 - \gamma_i$, are ~0, 0.07, 0.14, 0.21, 0.27, 0.24, and 0.29, whereas the values for F^- and Cl^- are larger, 0.39 and 0.44. These γ_i's can be compared with those estimated from the experimental S_N2 gas phase barriers in the preceding section. For group VI the average here of γ_i of about 0.25 compares with values there of a little under 0.2, and a value in this range might be used as a rough estimate in applications involving A_i^-'s of groups IV−VI.

Remarks on Computer Simulations. In a system with many coordinates, one task is that of finding the transition state hypersurface, and thereby a suitable reaction coordinate. In the case of weak overlap electron transfer reactions the energy difference ΔU between the products' and the reactants' potential energy[10,31] has been a useful reaction coordinate and has permitted the definition of the transition state as a particular hypersurface in the space.[10,31−33] However, in atom or group transfers particular care is needed. This energy difference can be a misleading coordinate, not so much near the TS, where the ΔU between the zeroth-order states is zero, but away from the TS, for example if the shape of the ΔG_r plot *vs* the reaction coordinate is being investigated, as it often is.

Such a difficulty can occur when the contribution ΔU_e of only the (x_1, x_2) terms [$U(x_1,x_2)$ for products minus $U(x_1,x_2)$ for reactants] is not monotonic along the expected reaction path in the (x_1, x_2) space. (Such a situation appears to have occurred at small A_1B distances in ref 33, perhaps arising from the difficulty noted there of accurately describing the $A_2B^-\cdots A_1$ repulsion.) To avoid this problem, and to learn about the λ_0 in the various ΔG_r and ΔG_p expressions away from the TS, one can introduce there a new coordinate ΔU_s, the difference in U due to all but the above (x_1, x_2) terms, and calculate $G_r(x_1,x_2,\Delta U_s)$ and G_p $(x_1,x_2,\Delta U_s)$ as functions of ΔU_s, x_1, and x_2. From this information λ_0 can be obtained: at $x_1 = 0$, $x_2 = \infty$, $G_p - G_r$ equals $\lambda_0 + \Delta G^{\circ\prime}$, so yielding λ_0 for the reactants, while at $x_1 = \infty$, $x_2 = 0$, $G_r - G_p$ equals $\lambda_0 - \Delta G^{\circ\prime}$, so yielding λ_0 for the products. These λ_0's in the reactants' region and in the products' are unambiguously known, since the two distinct charge distributions are known. However, in the TS region questions such as the validity of a two-state approximation arise and complicate a two-charge distribution description (next subsection), particularly when β is large.

Some quantum chemistry calculations have been performed seeking for a gas phase system specific transition state configurations for S_N2 and ET reactions, (e.g., ref 34). The TS for the ET reaction, however, has a much broader definition than a saddle-point, because of the "looseness" of the TS. It would be useful, therefore, to explore the entire TS region, e.g., the dotted line in Figure 1a near and between the S_N2 and ET arrows. In the process, a broader definition of TS than a saddle-point is used, and the solvent is included, using near the TS the ΔU as a reaction coordinate. Perhaps it may be possible in the process to extend or examine some existing S_N2 trajectory studies in solution[35] to include the ET portion of the TS and the region in between. The question of whether the flux density across this TS is bimodal or unimodal could be explored, for example.

We also note that simulations can shed light on the relative importance of the various terms in the equations for ΔG_r, as well as in testing some empirical form such as that in Appendix A, perhaps with a different p_i there for the electronic and

solvation terms. The functional form of model in Appendix A, or the corresponding form for neutrals, can be tested via only its consequences, since a concrete definition of n_i in terms of actual coordinates was not given or needed.

Nonequilibrium Polarization. We consider next the evaluation of the solvent reorganization energy portion of the energy barrier to reaction, the $\lambda_0/4$ in eq 16. We recall the origin of this barrier, which is different from that due to a desolvation of A_2^- in reaction 3 or 4: The slow moving solvent molecules cannot be appropriately aligned to the instantaneous position of the electronic charge in $A_1BA_2^-$. Thereby, the set of nuclear configurations adjusts, instead, to some averaged charge distribution of the electrons in $A_1BA_2^-$. One main problem is then how to treat the correlation between the electrons in $A_1BA_2^-$ and those of the solvent.[36] The treatment of that correlation, together with finding the nonequilibrium distribution of positions of the nuclei of the solvent, was the main focus in the electron transfer theory.[11b]

When the "frequencies" (energy level differences, in units of h) of the electronic motion in $A_1BA_2^-$ and in the solvent are comparable, the attractive electron correlation is described via London dispersion forces (second-order perturbation theory). In the present problem there are a variety of relevant electronic "frequencies" of $A_1BA_2^-$. One electronic frequency in the TS of $A_1BA_2^-$ is that associated with the splitting $\Delta\epsilon$ of the two states there and is the frequency $\upsilon = \Delta\epsilon/h$ for the electronic oscillation that would occur in a time-dependent electronic oscillation problem, $A_1^-BA_2 \leftrightarrow A_1BA_2^-$ or $A_1^{+\delta-1}B^{-\delta}A_2 \leftrightarrow A_1B^{-\delta}A_2^{\delta-1}$, where δ may be positive or negative. Another frequency, roughly speaking, is that associated with electronic transition within each A_i^- to an excited electronic state of A_i^-, the electronic "frequency" being $\Delta E/h$. It is large and more or less comparable with the solvent electronic frequencies. Any detailed treatment of the electron correlation should not be confined to a two-state model, particular when β is large. In a more realistic description one would solve the many-electron correlation problem directly, not making any two-state prejudgement. However, except when the excess electron in $A_1BA_2^-$ can be regarded as "slow", the problem is formidable.

We recall here only a two-state model, in which we assume in addition the electron to be "slow". Using statistical mechanical results in ref 37 and 22, based on a linear response approximation [the quadratic dependence on Y in eqs 5 and 6], it will be recalled that the free energy of a nonequilibrium polarization term λ_0 was given by eq 22. The "0" in eq 22 refers to the charge distribution of the solute which determines the distribution of nuclear coordinates of the solvent in the TS. This ρ_0 is, in the TS state, approximately equal to $^1/_2(\rho_{A_1} + \rho_{A_2})$ in a two-state approximation if electronic overlap is neglected; ρ_{A_i} is the charge density if the electron were concentrated on A_i^- or A_iB^-; that is, this ρ_0 is distributed equally between the A_1 and A_2 regions. The "1" in eq 22 refers to the actual charge distribution, which, in the present instance, for the TS is ρ_{A_1} when the electron is in the vicinity of A_1 and is ρ_{A_2} when in the vicinity of A_2. Thus, ρ_{1-0} is approximately $^1/_2(\rho_{A_1} - \rho_{A_2})$ in the vicinity of A_1 and $^1/_2(\rho_{A_2} - \rho_{A_1})$ in the vicinity of A_2, for this case, where both A_1^- and A_1^- bear a single negative charge in reaction 3. Thereby, $1-0$ corresponds to there being a hypothetical charge of $-e/2$ on A_1 and $-e/2$ on A_2^-.

Purely for illustrative purposes an oversimplified two-sphere model is next used for the present system, in conjunction with a dielectric continuum model, ΔG_{sol}^{ne}. The expression for $G_{1-0}^{e,sol}$ is then $-(e^2/4)(1/2a_1 + 1/2a_2 - 1/R)(1 - \epsilon_s^{-1})$ and that for $G_{1-0}^{solv}(op)$ is $(-e^2/4)(1/2a_1 + 1/2a_2 - 1/R)(1 - \epsilon_{op}^{-1})$, where ϵ_s and ϵ_{op} are the static and optical dielectric constants of the solvent. Thereby, the free energy barrier ΔG_{sol}^{ne} would be $(e^2/4)(1/2a_1 + 1/2a_2 - 1/R)(\epsilon_{op}^{-1} - \epsilon_s^{-1})$, the well-known expression for $\lambda_0/4$. More general continuum expressions, with a more realistic geometry, could be used instead. Still, more generally, one could use a statistical mechanical calculation to obtain G_{1-0}^{sol} and $G_{1-0}^{sol}(op)$, rather than a continuum expression.

For the present purposes, we only need λ_0 in the TS region. If one wished to obtain λ_0 for any other (x_1, x_2) value, e.g., for a system in the encounter complex region R, instead of the TS, one could again use the above ideas to obtain the λ_0. For example, in the configuration R the "0" charge density has a negative charge on A_2 and none on A_1. In the "1" system, i.e., the $A_1^-BA_2$ system, there is a negative charge $-e$ on A_1 and none on A_2. Thus in a $1-0$ system, there is a charge of $-e$ on A_1 and $+e$ on A_2. The two-center model for λ_0 yields, using eq 22, $e^2(1/2a_1 + 1/2a_2 - 1/R)(\epsilon_{op}^{-1} - \epsilon_s^{-1})$, which is the usual expression for λ_0. In a somewhat more elaborate treatment of a "slow electron" in the $A_1B\ A_2^-$ TS, i.e., not a two-state model, one would solve its one-electron Schrödinger, taking into account its instantaneous interaction of the electron with the nuclei and with the electrons of the solvent. However, for systems with a large β in the TS region, this electron is not "slow", and a more elaborate and non-two-state description needs to be explored.

IV. Summarizing Remarks

We have explored a molecular two-interacting-states model (and in Appendix A a modified BEBO-like one) for S_N2 reactions of the ET type, have extended slightly a model for outer sphere ET/bond rupture reactions, and introduced a unified description of the two, as in eqs 37a and 36b. The question of bimodal *vs* unimodal flux density for crossing the transition state (hypersurface) is also discussed, together with some data that may relate to this question. Estimates were made of entropies of activation for two limiting situations (loose and tight TS), and were also considered in relation to the data on S_N2 *vs* concerted ET/bond rupture paths. Variational calculations taking into account the dependence of the TS partition function $Q^\dagger$ on a variational parameter (e.g., X_2) can be used to implement the unified description. Other topics considered were the cross-relation, effect of driving force, leaving group, relative rates of S_N2 and ET/bond rupture paths, and a possible expediting of the ET/bond rupture by an incipient S_N2 interaction. Various numerical results were used to estimate a resonance energy parameter γ_i.

Acknowledgment. It is a pleasure to acknowledge the support of this research by the National Science Foundation and the Office of Naval Research. The author has benefitted considerably from an extensive correspondence with Jean-Michel Savéant. I am also particularly indebted to John Brauman, Henning Lund, Sason Shaik, and Lennart Eberson for their helpful comments.

Appendix A. Adiabatic Model

In his BEBO model for S_N2 reactions of neutrals, Johnston[7] obtained (in a more detailed molecular version) a consistency with experimental activation energies to about ± 2 kcal mol^{-1}. His method (constant bond order) is consistent with (and perhaps motivated by) the fact that the activation energies of the thermoneutral reactions are considerably less than the energy of the bond being broken. The latter result could be construed as implying an approximate constancy of "bond order" during the reaction. In the extension here to S_N2 reactions in solutions,

a simple functional form, related to that in one version of Johnston's approach, is adopted, but now no longer involving only bond energies. Electron affinities and solvation free energies also appear, and the "bond order" is replaced by a reaction coordinate. The three effects (i−iii) in the Introduction are again included, the solvation effect (iii) via a partial desolvation.

In a BEBO treatment[7] of gas phase reactions the bond order of the rupturing bond in the reactants was denoted by n_1, that of the newly forming bond by n_2, and the energy of the A_iB bond ($i = 1, 2$) relative to vacuum by V_i. The V_i and n_i were related by[7]

$$V_i = D_i n_i^{1+p_i} \tag{A1}$$

where in the exponent p_i is a quantity whose value is in the vicinity of zero,[7] typically around 0.1. The p_i should be greater than zero, in order that V_i not be larger in magnitude than D_i in the interval $0 \le n_i \le 1$. Johnston[7] defined the reaction path by introducing a constant bond order approximation, namely,

$$n_1 + n_2 = 1 \tag{A2}$$

the physical justification for the latter being that implied earlier, namely, there is little change of electronic energy along the reaction path. In ref 7a a triplet repulsion between the distant groups, A_1 and A_2, was also included and played an important role. When it is neglected, p_i becomes an empirical parameter rather than being evaluated[7a] from spectroscopic data. The energy of the system along the reaction path relative to that of the reactants is then $V_1 + V_2 + D_1$, since initially $n_1 = 1$ and $n_2 = 0$.

In the case of bond energies and activation energies for neutrals, the smallness of the latter relative to the former in a thermoneutral reaction shows that the p_i in eq A1 must be close to zero: With a TS having $n_1 \cong n_2 \cong 1/2$, and with $D_1 \cong D_2$ (thermoneutral reaction) the energy barrier is $-2D_1(1/2)^{1+p_i} + D_1$, and so $(1 - 2^{-p_i})$ must be small and typically p_i is on the order of 0.1. In the present case, $(A_1\cdots B\cdots A_2)^-$ involves additional changes besides bond energies.

Quantities relevant to the reactants in reaction 3 are the election affinity $E_{A_i\bullet}$ of $A_i^\bullet$, the dissociation energy D_{A_iB} of A_iB, and the solvation free energy of the ion A_i^-, $-g_{A_i^-}$. Their contribution to the free energy of the system changes from $-D_{A_1B} - E_{A_2\bullet} - g_{A_2^-}$ for the reactants to $-D_{A_2B} - E_{A_1\bullet} - g_{A_1^-}$ for the products. Each individual term in the sum may be large, and the sum even more so. The barrier to reaction is expected to be substantially less than this sum, and so for this reaction in solution one might consider modeling this contribution G of the free energy by an empirical expression of a form functionally similar to that in eq A1:

$$G = (-D_{A_1B} - E_{A_2\bullet} - g_{A_2^-})n_1^{1+p_1} + (-D_{A_2B} - E_{A_1} - g_{A_1^-})n_2^{1+p_2} \tag{A3}$$

The use of a single p_i for all the electronic and solvation effects is an assumption that we have introduced in eq A3 only for notational brevity. A simple modification for the case in which different p_i's are used for the solvation (g) and electronic terms ($-D - E$) is given later. With this expression both gas phase and solution phase barriers can be treated.

In eq A3 the p_i is different from that in eq A1 but is again close to zero, and eq A2 is still used. For example for the $Cl^- + CH_3Cl \rightarrow ClCH_3 + Cl^-$ reaction, the E_A, D_{AB} and g_A- are about 83, 84, and 77 kcal mol^{-1}, and so the sum is about 244 kcal mol^{-1}, whereas the energy barrier to reaction is about 26 kcal mol^{-1}, i.e., on the order of 10% of the sum.[4d] This percentage is higher for identity reactions for which in $A_iB + A_i^- \rightarrow A_i^- + BA_i$ the A_i^- is not a halide.

The source of the repulsion term is seen in Savéant's model[6] for concerted ET/bond rupture, eq 29, as well as in eqs 5 and 6. Because of the correlated nature of n_1 and n_2 in eq A2 and because of the omission of a triplet repulsion term, it should be stressed that one cannot assign the V_i term only to the A_iB bond: An increase in one bond length is accompanied by a decrease in the other, because of the correlation. Instead, the G in eq A3 is now only an empirical form, one which has several advantageous features listed below. Correspondingly we treat n_2 as a reaction coordinate and no longer as a bond order. The same remarks apply to the application to gas phase reactions.

One feature of eq A3 is that when p_i is close to zero the fractional change in G is relatively small, as observed experimentally in some reactions (particularly those of halides). A second feature is that eq A3 incorporates three effects mentioned earlier: with p_i close to zero, the terms yield the partial desolvation which accompanies the delocalization of charge over the entire $A_1BA_2^-$. The presence of the D_{A_iB} terms in eq A3 yields an increase in overall electronic energy, paralleling the repulsion in eqs 5 and 6, and the $E_{A\bullet}$ terms yield to an expected weaker electron affinity of $A_1BA_2^-$, compared with that of the smaller A_1^- or A_2^-. A third feature is that for identity reactions ($A_1 = A_2$) it makes the barrier for the reaction in solution larger than the gas phase barrier, as found experimentally and as discussed later. (The g terms in eq A3 are absent in the gas phase reaction.)

The quantities $E_{A_i\bullet} + g_{A_i-}$ are related to the standard electrode potentials $E^\circ_{A_i\bullet/A_i-}$ by

$$E_{A_1\bullet} + g_{A_i^-} - (E_{A_2\bullet} + g_{A_2^-}) = E^\circ_{A_2\bullet/A_2^-} - E^\circ_{A_1\bullet/A_1^-} \tag{A4}$$

Using the values of E, g, and E° for some known system, the sum $E_{A_i-} + g_{A_i-}$ can be obtained from the $E^\circ_{A_i\bullet/A_i-}$ for any other system.

The change of solvation from configurations appropriate to reactants to those appropriate to products is treated by the g terms in eq A3, whereas it is treated by the Y terms in eqs 5 and 6. The free energy G along the reaction path is given by

$$G = -\sum_{i=1,2} C_i n_i^{1+p_i} + n_1 w_r + n_2 w_p \tag{A5}$$

where

$$C_i = D_i + E_i + g_i \tag{A6}$$

$D_1 = D_{A_1B}$, $E_1 = E_{A_2\bullet}$, $g_1 = g_{A_2-}$, etc., and the w terms have been added to eq A5 to allow for the interactions at R (w_r, $n_1 = 1$) and at P (w_p, $n_2 = 1$) and to interpolate between them. Typically, one expects for reaction 3 that $w_r \cong w_p$. Then the last two terms in eq A5 reduce to w_r. However, that approximation is not made in eq A7 below.

Equation A5 reduces to the desired initial thermal equilibrium value at R and to the desired final equilibrium value at P. There is also some mean van der Waals' type solvation of the neutral A_1B and of A_2B, but we assume it to be roughly constant during the reaction, compared with changes in the usually larger ion-solvation and electronic terms.

From the preceding equations we obtain, starting at the given configuration R, the free energy change ΔG_r at any point (n_1, n_2) along the reaction path. It includes changes in electronic and solvational terms, but not in the ln Q terms in its definition.

The ΔG_r equals $G - (-G_1 + w_r)$, and eqs A5 and A6 then yield

$$\Delta G_r = \sum_{i=1,2} C_i n_i (1 - n_i^{p_i}) + n_2 \Delta G^{\circ\prime} \quad \text{(A7)}$$

where $\Delta G^{\circ\prime}$ is given by eq 9b and the second half of eq 7.

We next determine the transition state by setting $\partial \Delta G_r / \partial n_1 = 0$, subject to the constraint imposed by eq A2, i.e., setting $n_2 = 1 - n_1$ wherever it appears. We obtain

$$C_1[1 - (1 + p_1)n_1^{p_1}] - C_2[1 - (1 + p_2)n_2^{p_2}] = \Delta G^{\circ\prime} \quad \text{(A8)}$$

When $n_1 \cong n_2 \cong 1/2$, the first term in eq A5 is $(1/2)\sum_i C_i(1 - 2^{-p_i})$. When this barrier is small relative to $(1/2)\sum_i C_i$, i.e., relative to the mean of the initial and final solvation plus electronic terms, then p_i must be close to zero, and we may expand the first term in the right side of eq A7 about its value at $p_i = 0$, as in ref 7b for gas phase metathesis reactions. The above equations then yield

$$\Delta p_i C_i (1 + \ln n_i) = \Delta G^{\circ\prime} \quad \text{(A9)}$$

$$\Delta G_r = -\sum_{i=1,2} p_i C_i n_i \ln n_i + n_2 \Delta G^{\circ\prime} \quad \text{(A10)}$$

where the Δ in eq A9 indicates that the $i = 1$ term is to be subtracted from the $i = 2$ term. We could now proceed, as in ref 7b, to simplify eqs A9 and A10 by symmetrizing them, so leading to a functional form for ΔG_r similar to the tanh expression there. Instead, we shall for our immediate purposes expand the equations about $n_1 = n_2 = 1/2$. Upon writing $n_1 = (1/2) - x$, $n_2 = (1/2) + x$, and expanding the right-hand side of eq A10 in powers of x, up to and including x^2, we have $\Delta G_r = A + Bx + Cx^2 + ...$, where $A = (1/2)[(p_1C_1 + p_2C_2)\ln 2 + \Delta G^{\circ\prime}_{RP}$, $B = \Delta G^{\circ\prime} + (p_1C_1 - p_2C_2)(1 - \ln 2)$ and $C = -(p_1C_1 + p_2C_2)$. To obtain x and hence n_1 and n_2 in the TS for any $\Delta G^{\circ\prime}_{RP}$, we can either make the same approximation to eq A9 or, equivalently, minimize ΔG_r with respect to x, yielding $n_2 - 1/2 = x = -B/2C$, and hence $\Delta G_r^* = A - B^2/4C$, i.e.,

$$\Delta G_r^* \cong \frac{\lambda}{4} + \frac{\Delta G^{\circ\prime}}{2} + \frac{\Delta G^{\circ\prime 2}}{2\lambda/\ln 2} \quad \text{(A11)}$$

plus higher order terms. In eq A11 the $\Delta G^{\circ\prime 2}$ is really an approximation to B^2, as described below. The λ in eq A11 is defined by

$$\lambda = (2 \ln 2)\sum_i p_i C_i \quad \text{(A12)}$$

Introducing the values for C_1 and C_2, we note that

$$C_1 = D_{A_1B} + E_{A_2\cdot} + g_{A_2^-}, \quad C_2 = D_{A_2B} + E_{A_1\cdot} + g_{A_1^-} \quad \text{(A13)}$$

C_1 also describes the change in electronic energy and solvation free energy of the reaction which would accompany any actual passage of an electron into the gas phase (apart from a small surface potential term of 0.1−0.2 eV).[22a]

$$A_2^- + A_1B \rightarrow e + A_2^\bullet + A_1^\bullet + B^\bullet \quad \text{(A14)}$$

where e is in the gas phase and A_2^- is solvated. C_2 describes the energy change in reaction A14 when the 1 and 2 there are permuted. We have noted that the $\Delta G^{\circ\prime 2}$ in eq A11 is really B^2, defined above. However, typically, if $p_i \cong 0.1$, the $(p_1C_1 - p_2C_2)(1 - \ln 2)$ in β becomes $0.03\Delta G^{\circ\prime}$ and may then be neglected relative to $\Delta G^{\circ\prime}$.

We consider next the interpretation of some experimental results with the model. The difference in solution phase and gas phase barriers in that model is $g_{A_i}p_i \ln 2$. A $p_i \ln 2$ of 0.2 for this term would yield 21, 15, 14, and 12 kcal mol^{-1} for this difference, for F^-, Cl^-, Br^-, and I^-, respectively, compared with the experimental values of 19(?), 17, 13, and 16(?), respectively. On the other hand a value of $p_i \ln 2$ of 0.07 for the gas phase barriers yields 13, 12, 10, and 9, respectively, compared with experimental values of 13(?), 10, 11, and 6(?). If $p_i \ln 2$ were assigned an intermediate value, 0.11, rather than using two (0.2 for the solvation and 0.07 for the electronic contribution), the solution phase barriers would be 34, 27, 24, and 21 kcal mol^{-1}, which are close to the experimental values listed above, but the above arguments suggest that the solvation p_i and the electronic p_i differ. The arguments made in the text regarding groups such as OH^- and CN^- would imply a p_i of 0.18 instead of 0.11. In particular, a p_i of 0.18 instead of 0.11 would be needed to obtain the observed 42 and 51 kcal mol^{-1} for the OH^- and CN^- reactions.

If different p_i's were used for the solvation (p_i^S) and electronic (p_i^e) terms, then eq A11 would still apply, but eq A12 would now read

$$\lambda = (2 \ln 2)[p_1^e(D_{A_1B} + E_{A_2\cdot}) + p_1^S g_{A_2^-} + p_2^e(D_{A_2B} + E_{A_1\cdot}) + p_2^S g_{A_1^-} \quad \text{(A15)}$$

References and Notes

(1) (a) Eberson, L. *Electron Transfer Reactions in Organic Chemistry*, Springer-Verlag: New York, 1987. (b) More recent analyses are given in: Eberson, L.; Shaik, S. *J. Am. Chem. Soc.* **1990**, *112*, 4484. Eberson, L. *New J. Chem.* **1992**, *16*, 151. (c) Pioneering work in such applications is given by Albery, W. J.; Kreevoy, M. M. *Adv. Phys. Org. Chem.* **1978**, *16*, 87. Albery, W. J. *Annu. Rev. Phys. Chem.* **1980**, *31*, 277. Kreevoy, M. M.; Ostovic, D.; Lee, I. S. H.; Binder, D. A. S.; King, G. W. *J. Am. Chem. Soc.* **1988**, *110*, 524. (d) Eberson, L. *Acta Chem. Scand.* **1984**, 439.

(2) (a) Savéant, J.-M. *Acc. Chem. Res.* **1993**, *26*, 455. Savéant, J.-M. *Tetrahedron* **1994**, *50*, 10117. (b) Savéant, J.-M. *Adv. Phys. Org. Chem.* **1990**, *26*, 1. (c) Lexa, D.; Mispelter, J.; Savéant, J.-M. *J. Am. Chem. Soc.* **1981**, *103*, 6806. (d) Andrieux, C. P.; Gallardo, I.; Savéant, J.-M. *J. Am. Chem. Soc.* **1986**, *108*, 638.

(3) (a) Lund, H.; Daasbjerg, K.; Lund, T.; Pedersen, S. U. *Acc. Chem. Res.* **1995**, *28*, 313. (b) Lund, T.; Lund, H. *Acta. Chem. Scand.* **1988**, *B42*, 269; *Acta Chem. Scand.* **1986**, *B40*, 470.

(4) (a) Shaik, S. S.; Schlegel, H. B.; Wolfe, S. *Theoretical Aspects of Physical Organic Chemistry. The S_N2 Mechanism*; Wiley-Interscience: New York, 1992. These authors also describe a two-state model, different in its quantitative form from the present one. See also ref 13 below. (b) Pross, A. *Theoretical and Physical Principles of Organic Reactivity*; Wiley-Interscience: New York, 1995. (c) Pross, A. *Adv. Phys. Org. Chem.* **1985**, *21*, 99. (d) Reference 4a, pp 144, 155, 164, 166. (e) Reference 4a, p 167.

(5) Lewis, E. S. *J. Am. Chem. Soc.* **1989**, *111*, 7576. Lewis, E. S. *J. Phys. Org. Chem.* **1990**, *3*, 1. Lewis, E. S.; Douglas, T. A.; McLaughlin, M. L. *Adv. Chem. Ser.* **1987**, *215*, 35. Lewis, E. S. *J. Am. Chem. Soc.* **1985**, *107*, 6668. Niyazymbetov, M. E.; Zhou, R. F.; Evans, D. H. *J. Chem. Soc., Perkins Trans. 2* **1996**, 1957. Cf. Lewis, E. S. *J. Phys. Chem.* **1986**, *90*, 3756. Lewis, E. S.; Hu, D. D. *J. Am. Chem. Soc.* **1984**, *106*, 3292.

(6) Savéant, J.-M. *J. Am. Chem. Soc.* **1987**, *109*, 6788.

(7) (a) Johnston, H. S. *Gas Phase Reaction Rate Theory*; Ronald Press: New York, 1966. Parr, C.; Johnston, H. S. *J. Am. Chem. Soc.* **1963**, *85*, 2544. Johnston, H. S. *Adv. Chem. Phys.* **1960**, *3*, 131. (b) Marcus, R. A. *J. Phys. Chem.* **1968**, *72*, 891, with a minor notational change: the $p_i + 1$ here is denoted by p_i there. (c) Cf. Agmon, H.; Levine, R. D. *Chem. Phys. Lett.* **1977**, *52*, 197. (d) In constructing potential energy surfaces using semiempirical calculations, Sato's work (Sato, S. *J. Chem. Phys.* **1955**, *23*, 2465) plays a significant role; cf. ref 7a, pp 58−62).

(8) Hebert, E.; Mazaleyrat, J.-P.; Welvart, Z.; Nadjo, L.; Savéant, J.-M. *Nouv. J. Chim.* **1985**, *9*, 75.

(9) Daasbjerg, K.; Christensen, T. B. *Acta Chem. Scand.* **1995**, *49*, 128.

(10) Marcus, R. A. *Discuss. Faraday Soc.* **1960**, *29*, 21.

(11) (a) For example: Marcus, R. A.; Sutin, N. *Biochim. Biophys. Acta* **1985**, *811*, 265; *Comments Inorg. Chem.* **1986**, *5*, 119. (b) Marcus, R. A. *J. Chem. Phys.* **1956**, *24*, 966. (c) Marcus, R. A. *J. Phys. Chem.* **1963**, *67*, 853, 2889.

(12) For example: Wladkowski, B. D.; Brauman, J. I. *J. Phys. Chem.* **1993**, *97*, 13158. Pellerite, M. J.; Brauman, J. I. *J. Am. Chem. Soc.* **1983**, *105*, 2672; *J. Am. Chem. Soc*. **1980**, *102*, 5993. Dodd, J. A.; Brauman, J. I. *J. Am. Chem. Soc.* **1984**, *106*, 5356. Dodd, J. A.; Brauman, J. I. *J. Phys. Chem.* **1986**, *90*, 3559. Staneke, P. O.; Groothuis, G.; Ingemann, S.; Nibbering, N. M. M. *J. Phys. Org. Chem*. **1996**, *9*, 471. De Puy, C. H.; Gronert, S.; Mullin, A.; Bierbaum, V. M. *J. Am. Chem. Soc.* **1990**, *112*, 8650. Barlow, S. E.; Van Doren, J. M.; Bierbaum, V. M. *J. Am. Chem. Soc.* **1988**, *110*, 7240. As pointed out by Brauman and co-workers, the calculations of the gas phase reaction barriers from the experimental data take into account the multiple transition states.

(13) A two-state model has been proposed for S_N2 reactions in Shaik, S. *J. Am. Chem. Soc*. **1981**, *103*, 3692. Shaik, S. *Nouv. J. Chim*. **1982**, *6*, 159. Shaik, S. *Acta Chem. Scand.* **1990**, *44*, 205. Shaik, S.; Hiberty, P. C. *Adv. Quantum Chem.* **1995**, *26*, 99. The ET and S_N2 mechanisms are regarded (for example, in the last reference) as competing on the same potential energy surface along different reaction coordinates (Figure 8 there). The two-state model is also summarized in ref 4a.

(14) Bernardi, F.; Paleolog, S. A. H.; McDonall, J. J. W.; Robb, M. A. *J. Mol. Struct. (THEOCHEM)* **1986**, *138*, 23.

(15) Lexa, D.; Savéant, J.-M.; Su, K.-B.; Wang, D.-L. *J. Am. Chem. Soc.* **1988**, *110*, 7617.

(16) Savéant, J.-M. *J. Am. Chem. Soc.* **1992**, *114*, 10595.

(17) Lee, W. T.; Masel, R. I. *J. Phys. Chem.* **1966**, *100*, 10945.

(18) Wentworth, W. E.; George, R.; Keith, H. *J. Chem. Phys.* **1969**, *51*, 1791. Wentworth, W. E.; Becker, R. S.; Tung, R. *J. Phys. Chem.* **1967**, *71*, 1652.

(19) Marcus, R. A. *J. Chem. Phys.* **1965**, *43*, 679.

(20) (a) Glasstone, S.; Laidler, K. J.; Eyring, H. E. *The Theory of Rate Process*; McGraw-Hill, New York, 1941. (b) In a bimolecular reaction between A and B three translations of the relative motion of the two reactants are transformed into two rotations, with a moment of inertia, $\mu\sigma^2$, σ being the separation distance and μ a reduced mass, and into the radial motion. As a result, one part of the TS expression for the rate constant, which is written in terms of partition functions, is $(k_BT/h)(8\pi^2\mu\sigma^2k_BT/h^2)/(2\pi\mu k_BT/h^2)^{3/2}$, which equals $(8\pi k_BT/\mu)^{1/2}\sigma^2$. We denote it by Z, a "collision frequency". Thus, one can define a reorganizational contribution to the free energy barrier, the ΔG^* in earlier papers and in eqs 15 and 20, and distinguish it from the conventional free energy of activation $\Delta G^\dagger$ defined via $k = (k_BT/h)\exp(-\Delta G^\dagger/k_BT$. (c) For $q_{rot}^{(2)}/q_{trans}^{(2)}$, i.e., $(8\pi^2\mu\sigma^2k_BT/h^2)/(2\pi\mu k_BT/h^2)$, we see that it equals $4\pi\sigma^2$ if the μ's are the same. An instructive alternative route to this result is to note that the momentum phase space integrals cancel in the numerator and denominator, and the ratio of the coordinate integrals is $\sigma^2\int\int \sin\theta\, d\theta\, d\varphi/\int\int dx\, dy$, where the denominator is over a unit area and the numerator yields $4\pi\sigma^2$. (d) For $q_{vib}^{(1)}/q_{trans}^{(1)}$, we have $(k_BT/h\nu)/(2\pi\mu k_BT)^{1/2}$, where ν is an effective frequency for motion within the solvent cage. If a "force constant" k and an amplitude a is introduced, then $\nu \cong (1/2\pi)(k/\mu)^{1/2}$, $ka^2/2 \cong k_BT$, and one finds $q_{vib}^{(1)}/q_{trans}^{(1)} = (\pi a^2)^{1/2}$. An instructive alternative route is to note that the momentum phase space integrals again cancel in the numerator and denominator, and the ratio of space integrals is $\int\exp(-kx^2/2k_BT)dx/\int dx$, where the denominator is unity (unit length). The result, $(2\pi k_BT/k)^{1/2}$, using the above value of k, again yields $(\pi a^2)^{1/2}$.

(21) For example: Enskog theory in: Egelstaff, P. A. *An Introduction to the Liquid State*, 2nd ed.; Clarendon Press: Oxford, 1992; p 273. Cf. Marcus, R. A. *Int. J. Chem. Kinet.* **1981**, *13*, 865.

(22) (a) von Burg, K.; Delahay, P. *Chem Phys. Lett.* **1981**, *78*, 287. Delahay, P. *Chem. Phys. Lett.* **1982**, *87*, 607. Takahashi, N.; Sakai, K.; Tanida, H.; Watanabe, I. *Chem. Phys. Lett*. **1995**, *246*, 183. (b) Marcus, R. A. *J. Chem. Phys.* **1965**, *43*, 1261. An equation related to the present eq 21, with λ_0 given by eq 22, but for charge transfer spectra rather than photoemission, is also derived there. (c) Relevant data on charge transfer spectra of anions in solution are given in: Loeff, I.; Treinin, A.; Linschitz, H. *J. Phys. Chem*. **1992**, *96*, 5264.

(23) Eberson, L. *Acta Chem. Scand.* **1982**, *B36*, 533. Ingold, C. K. *Q. Rev. Chem. Soc.* **1957**, *11*, 1.

(24) (a) Wolfe, S.; Mitchell, D. J.; Schlegel, H. B. *J. Am. Chem. Soc.* **1981**, *103*, 7694. Donnella, J.; Murdoch, J. R. *Ibid*. **1984**, *106*, 4724, and references cited therein. (b) Mitchell, D. J.; Schlegel, H. B.; Shaik, S. S.; Wolfe, S. *Can. J. Chem*. **1985**, *63*, 1642.

(25) Daasbjerg, K.; Hansen, J. N.; Lund, H. *Acta Chem. Scand.* **1990**, *44*, 711.

(26) (a) Daasbjerg, K.; Pedersen, S. U.; Lund, H. *Acta Chem. Scand.* **1991**, *45*, 424. (b) Balslev, H.; Daasbjerg, K.; Lund, H. *Acta Chem. Scand.* **1993**, *47*, 1221. (c) Jorgensen, L. V.; Lund, H. *Acta Chem. Scand.* **1993**, *47*, 577.

(27) Cf.: Walder, L., cited in ref 2b.

(28) Benson, S. W. *Thermochemical Kinetics*; John Wiley: New York, 1976. q_v is typically 1−10 and q_r 10−100 (p 143). The data for the $10^{8.6}$ average are given on p 156.

(29) Savéant, J.-M. Private communication.

(30) Chidsey, C. E. D. *Science* **1991**, *251*, 919; *Ibid.* **1991**, *252*, 631. Curvature of ln k *vs* $E°$ plots for a reaction at an electrode was first established in Savéant, J.-M.; Tesser, D. *Discuss. Faraday Soc.* **1982**, *74*, 57. Examples of curved ln k *vs* $E°$ plots at electrodes (using self-assembled monlayers) are: Richardson, J. N.; Peck, S. R.; Curtin, L. S.; Tender, L. M.; Terrill, R. H.; Carter, M. T.; Murray, R. W.; Rowe, G. K.; Creager, S. E. *J. Phys. Chem*. **1995**, *99*, 766. Forster, R. J.; Faulkner, L. R. *J. Am. Chem. Soc*. **1994**, *116*, 5444; *J. Am. Chem. Soc.* **1994**, *116*, 9411. Smalley, J. F.; Feldberg, S. W.; Chidsey, C. E. D.; Linford, M. R.; Newton, M. D.; Liu, Y. P. *J. Phys. Chem*. **1995**, *99*, 13141. Ravenscroft, M. S.; Finklea, H. O. *J. Phys. Chem.* **1994**, *98*, 3843. Feng, Z. Q.; Imabayashi, S.; Kakiuchi, T.; Niki, K. *J. Elec. Chem.* **1995**, *394*, 149.

(31) Churg, A. K.; Weiss, R. M.; Warshel, A.; Takano, *J. Phys. Chem.* **1983**, *87*, 1683. Warshel, A. *J. Phys. Chem.* **1982**, *86*, 2218.

(32) For example: Zichi, D. A.; Ciccotti, G.; Hynes, J. T.; Ferrario, M. *J. Phys. Chem.* **1989**, *93*, 6261. Carter, E. A.; Hynes, J. T. *J. Phys. Chem.* **1989**, *93*, 2184. Yoshimori, A.; Kakitani, T.; Enomoto, Y.; Mataga, N. *J. Phys. Chem*. **1989**, *93*, 8316. Tachiya, M. *J. Phys. Chem*. **1989**, *93*, 7050.

(33) Perez, V.; Lluch, J. M.; Bertran, J. *J. Mol. Liq*. **1994**, *60*, 147. Perez, V.; Lluch, J. M.; Bertran, J. *J. Am. Chem. Soc*. **1994**, *116*, 10117. Perez, V.; Gonzalez-Lafont, A.; Lluch, J. M.; Bertran, J. *J. Chem. Soc., Faraday Trans.* **1995**, *91*, 1451.

(34) Bertran, J.; Gallardo, I.; Moreno, M.; Savéant, J.-M. *J. Am. Chem. Soc.* **1996**, *118*, 5737.

(35) For example: Gertner, B. J.; Whitnell, R. M.; Wilson, K. R.; Hynes, J. T. *J. Am. Chem. Soc.* **1991**, *113*, 74. Truhlar, D. G.; Schenter, G. K.; Garrett, B. C. *J. Chem. Phys.* **1993**, *98*, 5756. Truhlar, D. G.; Lu, D. H.; Tucker, S. C.; Zhas, X. G.; Gonzalez-Lafont, A.; Truong, T. N.; Maurice, D.; Liu, Y. P.; Lynch, G. C. *ACS Symp. Ser*. **1992**, *502*, 16. Sastry, G. N.; Shaik, S. *J. Phys. Chem.* **1996**, *100*, 12241.

(36) Gehlen, J. N.; Chandler, D.; Kim, H. J.; Hynes, J. T. *J. Phys. Chem.* **1992**, *96*, 1748. An expansion of this work is given in: Mathis, J. R.; Bianco, R.; Hynes, J. T. *J. Mol. Liq.* **1994**, *61*, 81.

(37) Marcus, R. A. *J. Chem. Phys*. **1963**, *39*, 1734.